



A nestling-sized skeleton of *Edmontosaurus* (Ornithischia, Hadrosauridae) from the Hell Creek Formation of northeastern Montana, U.S.A., with an analysis of ontogenetic limb allometry

Mateusz Wosik, Mark B. Goodwin & David C. Evans

To cite this article: Mateusz Wosik, Mark B. Goodwin & David C. Evans (2018): A nestling-sized skeleton of *Edmontosaurus* (Ornithischia, Hadrosauridae) from the Hell Creek Formation of northeastern Montana, U.S.A., with an analysis of ontogenetic limb allometry, *Journal of Vertebrate Paleontology*, DOI: [10.1080/02724634.2017.1398168](https://doi.org/10.1080/02724634.2017.1398168)

To link to this article: <https://doi.org/10.1080/02724634.2017.1398168>



[View supplementary material](#)



Published online: 16 Feb 2018.



[Submit your article to this journal](#)



[View related articles](#)



[View Crossmark data](#)



ARTICLE

A NESTLING-SIZED SKELETON OF *EDMONTOSAURUS* (ORNITHISCHIA, HADROSAURIDAE) FROM THE HELL CREEK FORMATION OF NORTHEASTERN MONTANA, U.S.A., WITH AN ANALYSIS OF ONTOGENETIC LIMB ALLOMETRY

MATEUSZ WOSIK,^{*1} MARK B. GOODWIN,² and DAVID C. EVANS^{1,3}

¹Department of Ecology and Evolutionary Biology, University of Toronto, 100 Queen's Park, Toronto, Ontario, M5S 2C6, Canada, m.wosik@mail.utoronto.ca;

²Museum of Paleontology, University of California, 1101 Valley Life Sciences Building, Berkeley, California 94720, U.S.A., mark@berkeley.edu;

³Department of Natural History, Royal Ontario Museum, 100 Queen's Park, Toronto, Ontario, M5S 2C6, Canada, d.evans@utoronto.ca

ABSTRACT—The Hell Creek Formation preserves one of the most intensely studied late Cretaceous terrestrial fossil units. Over 22 dinosaur genera are currently recognized from this unit, but the record of juvenile individuals is surprisingly limited. Here, we document a nestling hadrosaur that represents the first occurrence of an articulated nestling dinosaur skeleton from the latest Cretaceous (late Maastrichtian) of North America. The specimen (UCMP 128181) preserves a partial scapula, nearly complete rib cage, vertebral series from the shoulder to mid-tail, a large portion of the pelvic girdle, and both hind limbs through a combination of bone and/or natural impressions in the concretion. It is assignable to the genus *Edmontosaurus* based on the shape of the prepubic process, or blade, of the pubis. The specimen represents the earliest ontogenetic growth stage of *Edmontosaurus* cf. *annectens* and possesses a femur length of 148 mm. It greatly contributes as a new end member to a sample of associated *Edmontosaurus* skeletons that is well suited for allometrically testing the hypothesized ontogenetic gait shift in hadrosaurs from bipedal juveniles to quadrupedal adults using individual limb proportions. Although UCMP 128181 does not preserve forelimbs, regressions based on associated *Edmontosaurus* skeletons ($N = 25$) reveal overall isometry of the forelimb relative to the hind limb, and within each limb. These data indicate that *Edmontosaurus* nestlings were anatomically capable of fully quadrupedal locomotion and provide no compelling evidence to support an ontogenetic gait shift in hadrosaurids.

SUPPLEMENTAL DATA—Supplemental materials are available for this article for free at www.tandfonline.com/UJVP

Citation for this article: Wosik, M., M. B. Goodwin, and D. C. Evans. 2018. A nestling-sized skeleton of *Edmontosaurus* (Ornithischia, Hadrosauridae) from the Hell Creek Formation of northeastern Montana, U.S.A., with an analysis of ontogenetic limb allometry. *Journal of Vertebrate Paleontology*. DOI: 10.1080/02724634.2017.1398168.

INTRODUCTION

The Hell Creek Formation has been intensely collected for over a century, making it one of the best-sampled late Cretaceous terrestrial units (e.g., Hartman, 2002; Pearson et al., 2002; Russell and Manabe, 2002; Horner et al., 2011; Lyson and Longrich, 2011; Clemens and Hartman, 2014; Scannella and Fowler, 2014; Fastovsky and Bercovici, 2016). At the turn of the 20th century, the early expeditions of Barnum Brown and others led to the first major dinosaur discoveries of the iconic *Tyrannosaurus*, *Triceratops*, and *Edmontosaurus* and established the Hell Creek strata as a rich source of vertebrate fossils from a critical period in Earth's history (Clemens and Hartman, 2014). To date, there are over 22 dinosaur genera representing both large- and small-bodied forms recognized from the formation (Russell and Manabe, 2002), with preservation ranging from articulated individuals (e.g., Brown, 1907; Garstka and Burnham, 1997) to multiple

bonebed occurrences (e.g., Christians, 1992; Colson et al., 2004; Mathews et al., 2009; Keenan and Scannella, 2014).

A recent dinosaur census of the Hell Creek Formation in northeastern Montana found that the horned dinosaur *Triceratops* was the most common dinosaur recovered as a skeleton from this well-sampled unit, and *Tyrannosaurus* was as common as the duck-billed *Edmontosaurus* (Horner et al., 2011). Juveniles of all taxa are surprisingly rare, with only *Triceratops* (Goodwin et al., 2006; Horner et al., 2011) and *Tyrannosaurus* (Hutchinson et al., 2014) known from multiple specimens spanning a relatively wide ontogenetic range. Small juvenile and perinatal individuals have only been reported on the basis of rare and highly fragmentary remains, albeit from the contiguous Lance and Frenchman formations (Carpenter, 1982; Tokaryk, 1997), and a dinosaur egg and egg shell have only recently been described (Jackson and Varriacchio, 2016).

The hadrosaurine hadrosaurid (sensu Xing et al., 2014, 2017) *Edmontosaurus annectens* is one of the most common dinosaur taxa from the Hell Creek Formation, yet it is known primarily from specimens representing later ontogenetic stages (Campione and Evans, 2011; Xing et al., 2014, 2017). The smallest and presumably youngest described ontogenetic morph (Goodwin and Evans, 2016) of *Edmontosaurus annectens* is LACM 23504, with a femur length approximately 40%

*Corresponding author.

Color versions of one or more of the figures in the article can be found online at www.tandfonline.com/UJVP.

of average adult size (Prieto-Márquez, 2014). Here, we present the smallest (estimated ~70 cm total body length) articulated skeleton of *Edmontosaurus* cf. *annectens*, UCMP 128181, discovered in 1980 by Harley Garbani in Garfield County, Montana. This specimen was briefly mentioned in Russell and Manabe (2002:173) but was neither illustrated nor described. This is the first record of an articulated nestling dinosaur skeleton from the Hell Creek Formation, and it greatly expands the known ontogenetic continuum for *Edmontosaurus*. The wide ontogenetic sample of this taxon permits the first allometric study of limb proportions in a hadrosaurid using associated skeletons and contributes new insights to the ongoing debate whether hadrosaurids underwent a gait shift from bipedality in juveniles to quadrupedality in adults (Dilkes, 2001).

GEOLOGICAL SETTING

University of California Museum of Paleontology (UCMP) locality V80092 is located on land managed by the Bureau of Land Management in Garfield County, Montana (Fig. 1). In situ and weathered bone originates from a series of stacked channels with multiple lag deposits in a complex of cut and filled cross-stratified channel sandstones in the upper Hell Creek Formation, about 10–15 m below the Z coal complex, which marks the top of the Hell Creek Formation in this general area (Sprain et al., 2015). Here, three different coals are separated by less than 1 m. The Hell Creek Formation exposures are extensive and characterized by white-weathering channel sandstones in the flats where abundant and often water-worn dinosaur bone is found, in addition to partly articulated turtles, crocodilian bones, and microvertebrate fossils. The sandstone is generally friable but can be locally cemented into ≤1 m elliptical-to-round, iron-cemented concretions. One of these concretions produced the articulated, nestling-sized skeleton, UCMP 128181, described here. Detailed locality information is on file at the UCMP. All permissions were obtained for land access, collecting, and curation of these fossils into the UCMP in 1980 and on additional visits by UCMP field crews in 1983 and 2016.

MATERIALS AND METHODS

Specimen UCMP 128181 is preserved in an ovoid sandstone concretion that measures ~60 cm on its long axis. The sandstone concretion was broken prior to collection into several larger pieces, some of which have been consolidated and glued back together. The main block (Fig. 2) hosts the largest portion of the specimen and consists of the majority of the right side of the skeleton. The counterpart (Fig. 3) is composed of several smaller pieces intentionally left separated and primarily comprises the left side of the skeleton. The extreme fragmentary nature of additional miscellaneous pieces associated with UCMP 128181 makes bone identification difficult, and they have been omitted from this description. The specimen was photographed using a Nikon D5300 DSLR camera with a Tamron AF 18–200 mm f/3.5–6.3 XR Di II LD Aspherical (IF) macro zoom lens (model A14NII), and interpretive outline drawings were executed in Adobe Illustrator CS6 by author M. W. In addition, a photogrammetric three-dimensional (3D) model was constructed using Agisoft PhotoScan version 1.2.6 and uploaded to MorphoSource as supplemental data (MorphoSource, Media Group M15342).

Measurements

For the allometric limb proportion study, appendicular measurements were gathered by the authors first hand, from

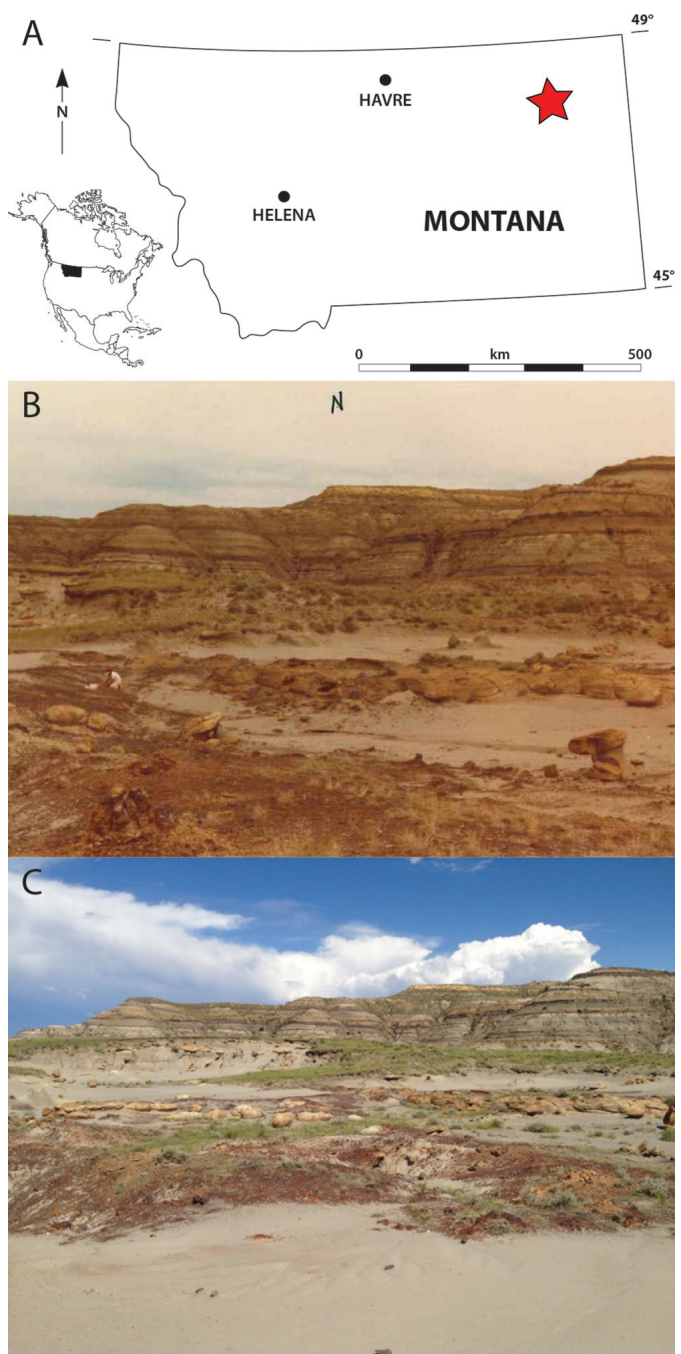


FIGURE 1. Sandstone basin UCMP locality V80092. A, geographic map of Montana, with the location where UCMP 128181 was discovered represented by a star; B, 1983 field photograph, with UCMP research paleontologist J. Howard Hutchison for scale; C, 2016 field photograph.

the published literature, and through the help of colleagues, from a total of 25 associated skeletons of *Edmontosaurus*, representing both *E. annectens* and *E. regalis* (Supplementary Data 1, Table S1). Linear measurements under 30 cm were taken with digital calipers, whereas those over 30 cm and all circumferences were taken using a fabric tape measure. Where data from left and right elements from the same specimen were taken, the measurements were averaged prior to the analyses. Data from specimens with a high degree of postmortem deformation (e.g., crushing, flattening) were

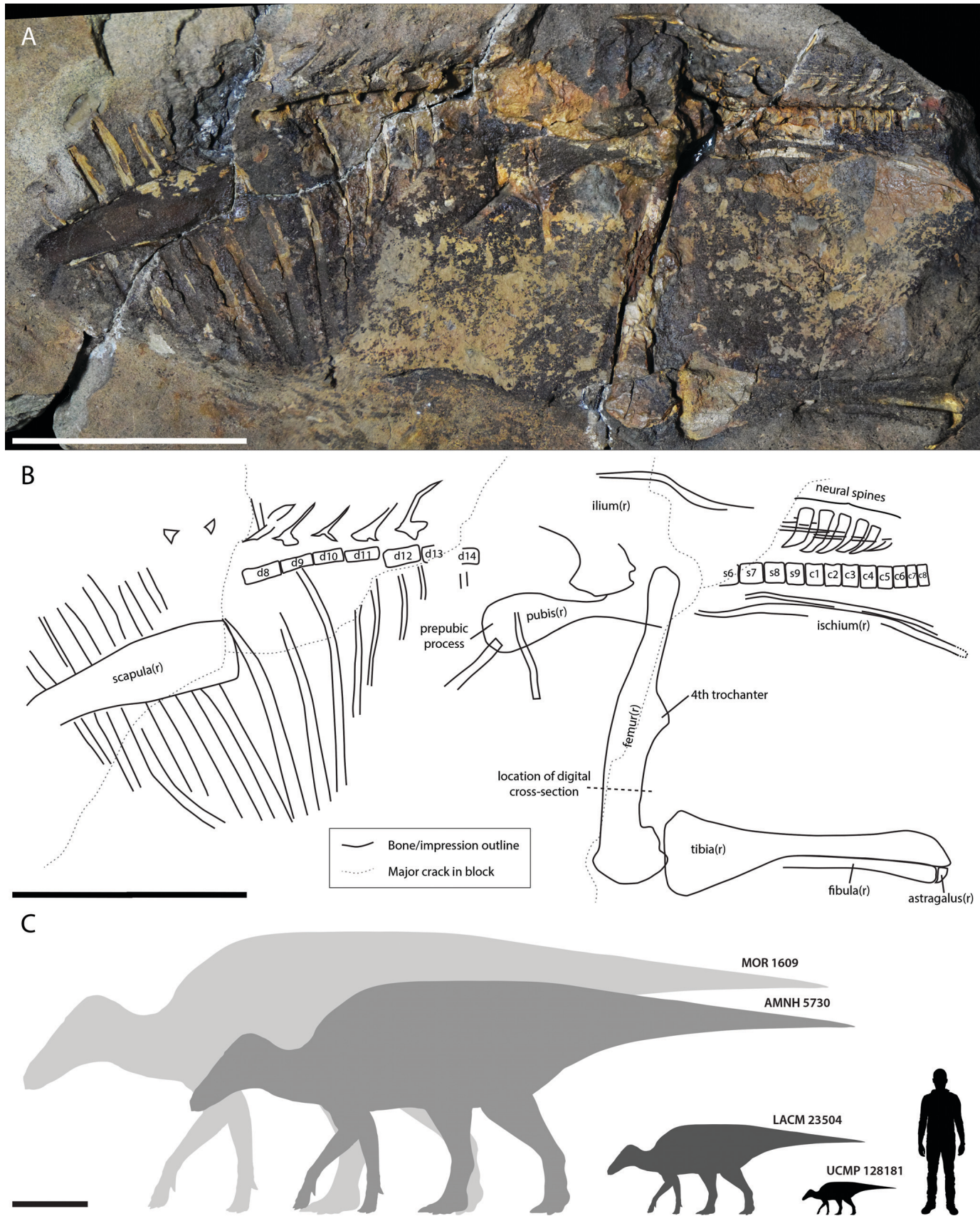


FIGURE 2. Main block of UCMP 128181 *Edmontosaurus* cf. *annectens* skeleton. **A**, specimen photo; **B**, digital outline of bone/impressions. Major bone elements are labeled along with orientation. Vertebrae correspond with actual location along vertebral column. **C**, estimated size of UCMP 128181 compared with the known ontogenetic series of *Edmontosaurus* cf. *annectens*. Silhouettes by D. Dufault. **Abbreviations:** **c**, caudal vertebra; **d**, dorsal vertebra; **(l)**, left; **(r)**, right; **s**, sacral vertebra. Scale bars equal 10 cm (**A** and **B**) and 1 m (**C**).

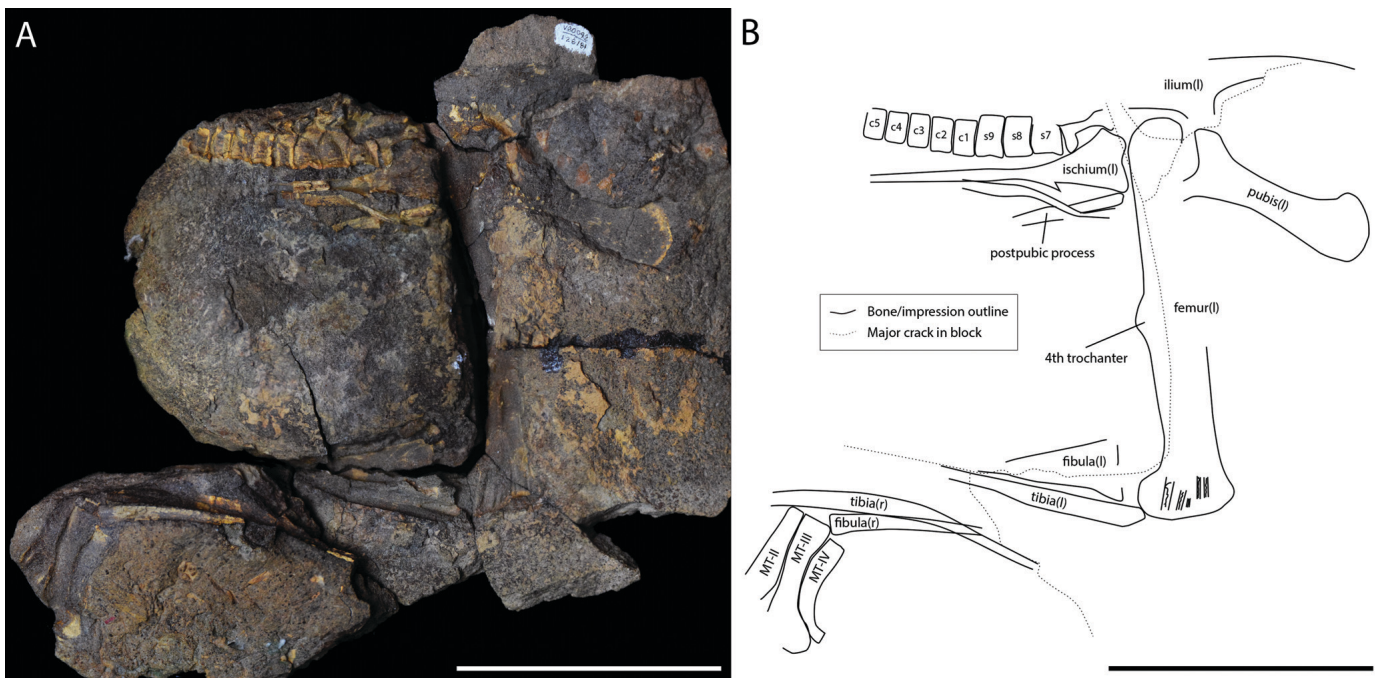


FIGURE 3. Counterpart of UCMP 128181 *Edmontosaurus* cf. *annectens* skeleton. **A**, specimen photo; **B**, digital reconstruction of bone/impressions. Major bone elements are labeled along with orientation. Vertebrae correspond with actual location along vertebral column. **Abbreviations:** **c**, caudal vertebra; **(l)**, left; **MT**, metatarsal; **(r)**, right; **s**, sacral vertebra. Scale bars equal 10 cm.

excluded from the analyses. Linear measurements of UCMP 128181 are included in Tables 1 and 2. The femur circumference of UCMP 128181 is incomplete and required estimation prior to the allometric analyses. The preserved half circumference of the right femur was measured using ImageJ 1.48v (Rasband, 1997) from a digital cross-section and doubled to produce an estimated minimum femur circumference of 60 mm for UCMP 128181. Results from the allometric analyses are reported in Tables 3 and 4. A summary of estimated values for missing elements of UCMP 128181 are listed in Table 5. Measurements of specimens used in the size comparison of perinatal and nestling hadrosaurs were gathered from the literature and are recorded in Table 6.

Institutional Abbreviations—**AMNH**, American Museum of Natural History, New York, New York, U.S.A.; **CCM**, Carter County Museum, Ekalaka, Montana, U.S.A.; **CMN**, Canadian Museum of Nature, Ottawa, Ontario, Canada; **CNMH**, Cleveland Museum of Natural History, Cleveland, Ohio, U.S.A.; **DMNH**, Denver Museum of Natural History, Denver, Colorado, U.S.A.; **FPDM**, Fukui Prefectural Dinosaur Museum, Katsuyama, Japan; **LACM**, Los Angeles Country Natural History Museum, Pasadena, California, U.S.A.; **MOR**, Museum of the Rockies, Bozeman, Montana, U.S.A.; **MPC**, Institute of Paleontology and Geology, Mongolian Academy of Sciences, Ulaan Baatar, Mongolia; **NCSM**, North Carolina Museum of Natural Sciences, Raleigh, North Carolina, U.S.A.; **NHMUK PV**, Natural History Museum, London, U.K.; **PIN**, Paleontological Institute, Russian Academy of Sciences, Moscow, Russia; **ROM**, Royal Ontario Museum, Toronto, Ontario, Canada; **SDSM**, South Dakota School of Mines and Technology, Rapid City, South Dakota, U.S.A.; **SM**, Senckenberg Naturmuseum, Frankfurt, Germany; **UCM**, University of Colorado Museum, Boulder, Colorado, U.S.A.; **UCMP**, University of California Museum of Paleontology, Berkeley, California, U.S.A.; **USNM**, Smithsonian National Museum of Natural History, Washington, D.C., U.S.A.;

UWBM, University of Washington Burke Museum, Seattle, Washington, U.S.A.; **YPM-PU**, Yale Peabody Museum of Natural History, New Haven, Connecticut, U.S.A.

Regression Analyses

The complete data set of *Edmontosaurus* linear measurements was analyzed for the allometric trajectories of 25 different appendicular comparisons to describe the best functional relationships among variables of the forelimb and hind limb and within each limb apparatus (Tables 3 and 4). These 25 comparisons were further subdivided to the species level and repeated by removing the nestling UCMP 128181 individual. The purpose of this subsampling was (1) to determine whether the relationships significantly changed when the overall data set was subsampled; and (2) whether the sole nestling specimen was potentially an outlier. Linear data were log-transformed prior to analysis using natural log (ln). Comparisons 1–15 were plotted against the reference datum, femur length, for the entire sample size. Femur length is an appropriate standard variable for this study because it is frequently used as a size proxy in allometric studies of the appendicular skeleton in terrestrial vertebrates, and unlike the forelimb, the hind limb is typically used in locomotion in terrestrial vertebrates (e.g., Campione and Evans, 2012). Standard (reduced) major axis (SMA or RMA; Tables 3 and 4) regressions were used to describe allometric relationships because they assume that both variables contain error from inaccurate measurements (Warton et al., 2006). Ordinary least squares (OLS; Supplementary Data 1, Tables S2 and S3) regressions were used to predict the size of missing or incomplete elements in UCMP 128181 (Warton et al., 2006), with femur length set as the standard variable, but these estimates were not included in any of the SMA analyses. This was particularly useful for determining an approximate size for the missing forelimb of the nestling individual (UCMP 128181). However, we do not use these estimates as primary data, but only to compare with forelimb–hind limb

TABLE 1. UCMP 128181 vertebral column measurements (mm).

Vertebra	Block	Length			Height		
		Dorsal	Middle	Ventral	Anterior	Middle	Posterior
d8	Main	15.9	15.6	15.1	9.1	7	9.6
d9	Main	15	14.4	13.7	10	7.3	7.6
d10	Main	15	14.3	15.3	>8.5	7.1	6.8
d11	Main	15.4	15	15.4	9.9	7.1	8.2
d12	Main	15.5	16.7	16	9.4	8.1	8.2
d13+d14*	Main	28*	29.8*	—	>8	—	9
s6	Main	—	11.2	>9.2	—	—	10.4
s7	Main	12	10.9	11.9	10.2	8.6	9.7
	Counterpart	>9.6	11.7	10.7	11.6	>9.5	13
s8	Main	10.8	10.3	10.5	9.5	8.3	9.1
	Counterpart	11.4	10.6	10.8	14	13.8	13.8
s9	Main	9.6	9.5	10.1	9.6	8.2	9.5
	Counterpart	9.2	9.5	10.2	13.8	13.1	13.8
c1	Main	9.2	8.2	9.3	9.3	8.6	9.3
	Counterpart	7.9	8.4	8.3	12.7	11.4	12.8
c2	Main	8.7	8	8.4	9.7	8.8	9.8
	Counterpart	7.9	7.9	8.5	12.3	10.9	12.1
c3	Main	8.5	8.1	8.6	10.3	10	11
	Counterpart	7.7	7.6	8	12.2	11.6	11.6
c4	Main	7.9	7.5	7.8	11.3	9.3	10.3
	Counterpart	7.9	7.3	7.9	11.7	10.4	12.5
c5	Main	7.7	6.5	7.1	9.7	9.1	9.4
	Counterpart	6.7	7.1	7.4	10.8	9.8	10.8
c6	Main	5.5	5.4	5.4	9.6	9.3	10.5
c7	Main	5.5	5.2	6.2	10.5	8.9	10.4
c8	Main	—	5.2	5.7	10.1	—	—

Numbering corresponds to actual location along vertebral column (Fig. 2, 3). Abbreviations: c, caudal; d, dorsal; s, sacral.

*Length measurements are summed because separation cannot be definitively distinguished.

ratios of articulated embryos and nestlings of other taxa as an external test of the feasibility of our allometric relationships. Table 5 contains summarized results in the form of percent (%) error taken as a ratio of the raw value to the OLS estimation. Slopes, intercepts, 95% confidence intervals, and correlation coefficients were determined for each comparison. Each comparison was evaluated using two-tailed p-values using a significance level of 0.05 for correlation between variables. Furthermore, the results of each regression were assigned as positively allometric (95% confidence interval of slope is greater than 1), negatively allometric (95% confidence interval of slope is less than 1), or isometric (95% confidence interval of slope includes 1). The regressions and statistical analyses were performed in R (R Development Core Team, 2016) with the package ‘lmodel2’ (Legendre, 2008).

Body Mass Estimation

The photogrammetric 3D model was digitally sectioned using Agisoft PhotoScan version 1.2.6 at the minimum diaphyseal circumference of the right femur between the fourth trochanter and distal end. In order to estimate the body mass of UCMP 128181, developmental mass extrapolation (DME) was used (Erickson and Tumanova, 2000). Body mass estimates were made on the basis of femur length and circumference measurements. The mounted CCM skeleton was used as the morphologically adult-sized individual in DME calculations.

SYSTEMATIC PALEONTOLOGY

ORNITHISCHIA Seeley, 1887

ORNITHOPODA Marsh, 1881

IGUANODONTIA Dollo, 1888

HADROSAURIDAE Cope, 1869

HADROSAURINAE Cope, 1869

EDMONTOSAURUS Lambe, 1917

EDMONTOSAURUS cf. *ANNECTENS* Marsh, 1892

DESCRIPTION AND ONTOGENETIC COMPARISON

Due to the nature of preservation, UCMP 128181 can only be described at a gross anatomical level. Most bones are preserved as natural molds, in which original bone is heavily fractured or is completely eroded away. Periosteal surfaces, delicate processes, and muscle scars are generally not preserved, particularly in the elements of the pelvic region. Fortunately, the primary dimensions (e.g., total lengths and widths) are easily measured and provided in Table 1 for vertebrae and Table 2 for the appendicular skeleton. For color figures, the reader is referred to the online version of this article. A 3D photogrammetric model of the main block is available online (MorphoSource, Media Group M15342).

Axial Skeleton

Dorsal Ribs—Fourteen dorsal ribs are preserved primarily as impressions in the main block, with varying degrees of preservation (Fig. 4). Starting with the anterior-most rib impression near the minimum constriction of the scapula, the length of the ribs increases to its longest just distal of this constriction and is succeeded by a dramatic reduction in length and robustness towards the final preserved rib impression. These progressively distinct features imply that the four missing dorsal ribs are those near the sacrum. It is not possible to determine the shape of the articulating ends.

Dorsal Vertebrae—Seven dorsal centra with incomplete posteriorly deflected neural spines are preserved primarily as impressions in the main block (Fig. 4). *Edmontosaurus* is reported to have 18–20 dorsal vertebrae (Gilmore, 1924; Lull and Wright, 1942). Assuming the anterior-most preserved dorsal rib impression represents the first dorsal rib, the first preserved dorsal centrum would be the eighth (d8). It is not possible to determine the shape of the faces of the centra or orientation of zygopophyses due to the specimen being preserved in medial orientation. However, the more anterior dorsal centra are longer and shallower and their lateral sides are less concave

TABLE 2. UCMP 128181 appendicular skeleton measurements (mm).

Element	Side	Dimension	Measurement (mm)
Scapula	R	Blade height	30.7
		Neck height	16.4
Ilium	R	Total length	>105
	R	Total length	>129
Pubis	R	Pubic blade to acetabular margin length	75.3
		Pubic blade height, distal	25.3
Ischium	L	Pubic blade height, minimum	114
	R	Total length	137
Femur	R	Total length	144
		Minimum circumference	30 ^b
Tibia	R	Midshaft diameter, maximum	19
		Midshaft diameter, minimum	15.5
Fibula	R	Medial condyle, anteroposterior width	33.2
		Fourth trochanter length	19.3
Metatarsal II	R	Fourth trochanter width	9.9
	L	Total length	150
Metatarsal III	R	Minimum circumference	30 ^b
	L	Lateral condyle, anteroposterior width	31.4
Metatarsal IV	R	Fourth trochanter length	18
		Total length	135.9
Tibia	R	Proximal width	39.5
		Midshaft width, minimum	9.9
Fibula	R	Total length	113
		Distal head width	8.9
Metatarsal II	L	Distal width	>41.7
		Shaft width, minimum	7.1
Metatarsal III	L	Total length	56.6
		Proximal width	14.5
Metatarsal IV	L	Distal width	17.1
		Shaft width, minimum	10
Metatarsal IV	L	Total length	>49.4
		Proximal width	10.3
Metatarsal IV	L	Shaft width, maximum	9.6
		Shaft width, minimum	4.2

^cEstimated length.^bHalf circumference.

anteroposteriorly than those centra closer to the sacrum, as in other hadrosaurs (Horner et al., 2004).

Sacral Vertebrae—The anterior end of the sacrum is either covered by sediment or eroded away, but the four posterior-most vertebrae of the sacrum are preserved in articulation with the first free caudal and identified as sacrals on the basis of fusion (Fig. 5). *Edmontosaurus* has nine fused sacrals (Lull and Wright, 1942), and following the conventional numbering of vertebrae, UCMP 128181 preserves sacrals 6 through 9. Fragmentary neural spines are canted posterodorsally and are preserved for these vertebrae (s8, s9), but the sacral ribs are not.

Caudal Vertebrae—Eight caudal centra with four accompanying neural spines are preserved primarily as impressions in the main block (Fig. 5A), whereas the counterpart preserves only five centra as impressions (Fig. 5B). We interpret the first free vertebra (c1) posterior to the fused sacral bar as the first caudal. Similar to the dorsal vertebrae, it is not possible to determine the shape of the articulating ends. The more anterior centra are longer and shallower, with stronger concave lateral sides than the more posterior centra, which expand slightly dorsoventrally and decrease to less than one-third of the size of the first caudal (Table 1). The base of the tail is straight and projects horizontally from the sacrum, as in other articulated skeletons of *Edmontosaurus* (Gilmore, 1924). The four posterodorsally deflected neural spines, three

of which are almost complete, exhibit an anteroposterior reduction in height and width distally along the tail. Several anteroposteriorly orientated ossified tendons overlap the neural spines in the region of the tail base.

Pectoral Girdle

Scapula—The right scapula is preserved posteriorly from the proximal neck constriction (Fig. 4). The scapula is represented by an impression in the main block that is lateral to the preserved ribcage, and the dorsal ribs have weathered away along with the scapula in this region. The scapula is a long (>88 mm) and arched bone with a weakly curved dorsal margin and a gradually dorsoventrally expanding distal blade. The disparity between the minimum dorsoventral height of the proximal constriction relative to the maximum dorsoventral height of the blade (~53%) is comparable to the juvenile LACM 23504 but is slightly greater than typical of adult specimens (>60%; Prieto-Márquez, 2014). The scapular blade terminates posteriorly at dorsal rib 7.

Pelvic Girdle

Ilium—The right and left ilia are preserved as impressions in the main block (Fig. 6A) and counterpart (Fig. 6C), respectively. The dorsal margin of the thin preacetabular process, visible on the main block, gently deflects ventrally towards its anterior end. The preacetabular process has a rounded anterior termination present on the counterpart but dives behind the matrix. The impression of the tall, posteriorly projecting postacetabular process has a possible weak dorsal expansion just anterior to its rounded posterior end. As preserved, the ilium is 105 mm in total length but is missing portions of both ends. The region above the acetabulum is dorsoventrally the tallest and the most robust portion of the ilium. There is a strong inflection in the dorsal margin above the acetabulum, as is characteristic of Hadrosauridae inclusive of *Bactrosaurus* and *Gilmoreosaurus* (Brett-Surman and Wagner, 2007). The counterpart contains an incomplete impression of the pubic peduncle, but it is difficult to distinguish between its ventral termination and the origination of the iliac peduncle of the pubis. The supraacetabular crest and ischial peduncle are not well preserved.

Pubis—Parts of the right and left pubes are well preserved as impressions in the main block and counterpart (Fig. 6), respectively. The right side has a virtually complete prepubic process (blade), with clear, complete margins except in the region adjacent to the acetabulum. Because of this, the iliac peduncle is difficult to discern from the origination of the pubic peduncle of the ilium, and the ischial peduncle is obscured by the femur. The height of the neck at the minimum constriction measures 11.4 mm, which is 45% of the maximum dorsoventral height of the expanded blade. In lateral view, the right pubis has a relatively long proximal constriction and a paddle-like, asymmetrical, and subellipsoidal anterior end that expands more ventrally than dorsally, as is typically observed in *Edmontosaurus* (e.g., CMN 2289, Campione, 2014; LACM 23504, Prieto-Márquez, 2014) and remains morphologically unchanged ontogenetically (Brett-Surman and Wagner, 2007; Prieto-Márquez, 2014). The long postpubic process is preserved as bone and is only visible on the counterpart. It is in natural position below the anterior end of the ischium and nearly parallels its ventral margin. The distal end of the postpubic process is broken, but a 129 mm portion of the left pubis is preserved.

Ischium—The triangular body of the left ischium is preserved as an impression on the counterpart (Fig. 6C). Although the dorsal and anterior terminations of the iliac and pubic peduncles are eroded away, the acetabular margin provides an estimate for the

orientation of each peduncle. This indicates that the ischium is preserved in natural articulation with the ilium and pubis. The iliac and pubic peduncles are quite similar to each other. Along the ventral margin of the ischial body, a broad obturator notch, preserved on the counterpart, is at least partially enclosed

posteriorly. In lateral view, the obturator notch is lenticular in shape, with the posterior end of the aperture more acute than the apparently poorly ossified anterior region. It is open, as expected in early ontogeny, and resembles the first stage of progressive ossification (Brett-Surman and Wagner, 2007). The



FIGURE 4. Anterior half of UCMP 128181 main block. **A**, overview containing dorsal ribs; **B**, close-up of right scapula. Scale bars equal 5 cm.



FIGURE 5. Tail impressions of UCMP 128181. **A**, main block; **B**, counterpart. Scale bars equal 5 cm.

caudal shafts of both ischia appear to be nearly complete distally, with rounded distal termini preserved as impressions, with fragments of bone on the main block (Fig. 2). The minimum expansion of the distal end of the ischium is consistent with *Edmontosaurus* and other hadrosaurines, and distinct from the expanded boot of lambeosaurines (Brett-Surman and Wagner, 2007). When the main block and counterpart are aligned, the left ischium is 137 mm long.

Hind Limb

Femur—The left (Fig. 7A) and right (Fig. 7B) femora are nearly complete and in articulation relative to the acetabulum. The right femur is composed of eroded bone in the main block and has a large dorsoventral crack permeating through it, whereas the left femur is represented by a detailed impression of the lateral side in the counterpart. The shafts of the femora are

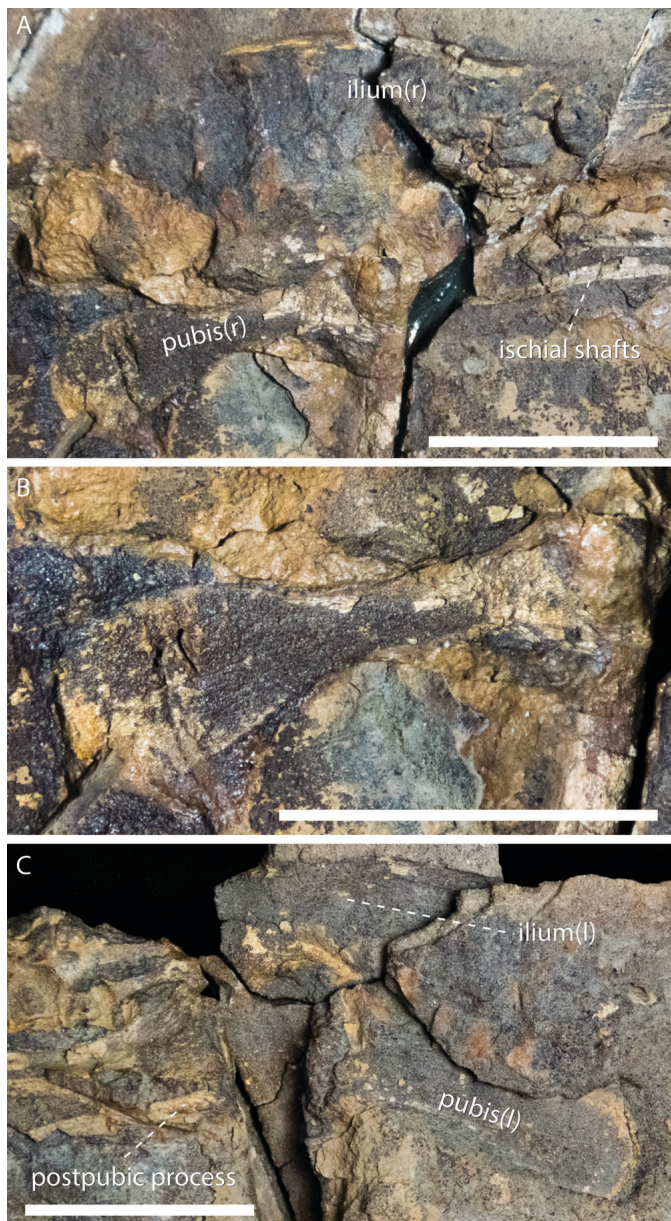


FIGURE 6. Pelvic girdles of UCMP 128181. **A**, main block; **B**, close-up of right pubis; **C**, counterpart. Scale bars equal 5 cm.

straight in medial view, but due to their orientation, it is difficult to determine whether there are any differences between the proportions of the proximal versus distal shaft regions. The fourth trochanter is positioned at approximately the midpoint of the diaphysis, as in adult hadrosaurids (Brett-Surman and Wagner, 2007), as well as juvenile and adult *Edmontosaurus annectens* (Prieto-Márquez, 2014) and *Maiasaura peeblesorum* (Guenther, 2014). The dorsal and ventral margins of the fourth trochanter preserve a symmetrical triangular outline in medial view, as seen in juveniles but not adults of *Edmontosaurus annectens* (Prieto-Márquez, 2014). The muscle attachment sites for the hind limb extensors and flexors, as well as the *m. gastrocnemius* and *m. tibialis anterior*, observed on the left femur occur in positions reported for other hadrosaurs (Dilkes, 2000), including *Edmontosaurus* (Maidment et al., 2014). The average total length of the femora is 148 mm, which is slightly longer than the ischium and

109% the length of the right tibia. The femur length compares to 26% of the LACM 23504 juvenile and 15% of the adult YPM-PU 2182.

Tibia—The right tibia is mostly preserved as an impression on the main block (Fig. 7C), whereas the left tibia only preserves a portion of the shaft as an impression in the counterpart. The tibia has a total length of 136 mm and is slightly shorter than the femur. The long axis of the proximal end, which includes the proximal condyles and the top of the cnemial crest, is oriented along an anterior-posterior plane, whereas the distal end is transversely oriented. The posterior end, which can be seen as an embossed impression, is preserved in the same plane as the surface of the main block, and the cnemial crest extends down the proximal third of the tibia. The diaphysis of the tibia is straight, and circular to triangular in cross-section. The distal end dives into the block; therefore, it is not possible to compare the robustness of the proximal and distal ends.

Fibula—The fibulae are incompletely preserved as impressions in the main block (Fig. 7C) and counterpart. The right fibula is articulated with the right tibia. The fibula is long and slender with an anteroposteriorly expanded distal head that is visible on the counterpart. The proximal head is the larger of the two ends in hadrosaurs but is not preserved in the main block because it articulates under the proximal half of the tibia. As a result, the total length of 113 mm for the right fibula was measured from the distal end of the fibula to the proximal end of the articulating tibia. The shaft is cylindrical in cross-section. Prieto-Márquez (2014) noted that the shaft becomes anteroposteriorly narrower towards the distal end during ontogeny. This may indicate that the cylindrical shape is characteristic of early ontogenetic stages.

Astragalus—The right astragalus is likely represented as an impression in the main block (Fig. 7C) in articulation with the right tibia, but is insufficiently preserved to be described in any detail.

Pes—Only the right metatarsus is preserved as an impression in the counterpart of the anterior side in articulation (Fig. 8). Metatarsal II preserves part of its proximal end but is incomplete distally. Metatarsal III is the largest in the series and preserves a complete total length of 56.6 mm. It has a slightly expanded proximal end relative to its diaphysis, which maintains a consistent diameter along much of its length. The region of the distal end in articulation with metatarsal II is not preserved but still provides enough evidence of a gradual mediolateral expansion directed distally. Metatarsal IV is the shortest in length (as preserved) and narrowest in maximum width among the three preserved tarsal elements. The proximal end originates just distal to the proximal end of metatarsal III and is distally incomplete.

Taxonomic Identification

Significant morphological changes occur during hadrosaurid ontogeny and occasionally hinder precise taxonomic identification of juvenile ontogimorphs (e.g., Evans et al., 2005; Guenther, 2009; Prieto-Márquez, 2011). Specimen UCMP 128181 is recognized as a hadrosaurine hadrosaurid (*sensu* Horner et al., 2004; Xing et al., 2014) based on a combination of ontogeny-independent characters (e.g., Evans et al., 2005; Brett-Surman and Wagner, 2007; Prieto-Márquez, 2011), or characters that do not significantly change with ontogeny in hadrosauroids. The minimum expansion of the distal end of the ischium is consistent with *Edmontosaurus* and other hadrosaurines and is distinct from the expanded boot of lambeosaurines (Horner and Currie, 1994; Brett-Surman and Wagner, 2007; Prieto-Márquez, 2010:character 271[0, slightly expanded into a blunt end]). The prepubic process has a relatively long, shallow proximal

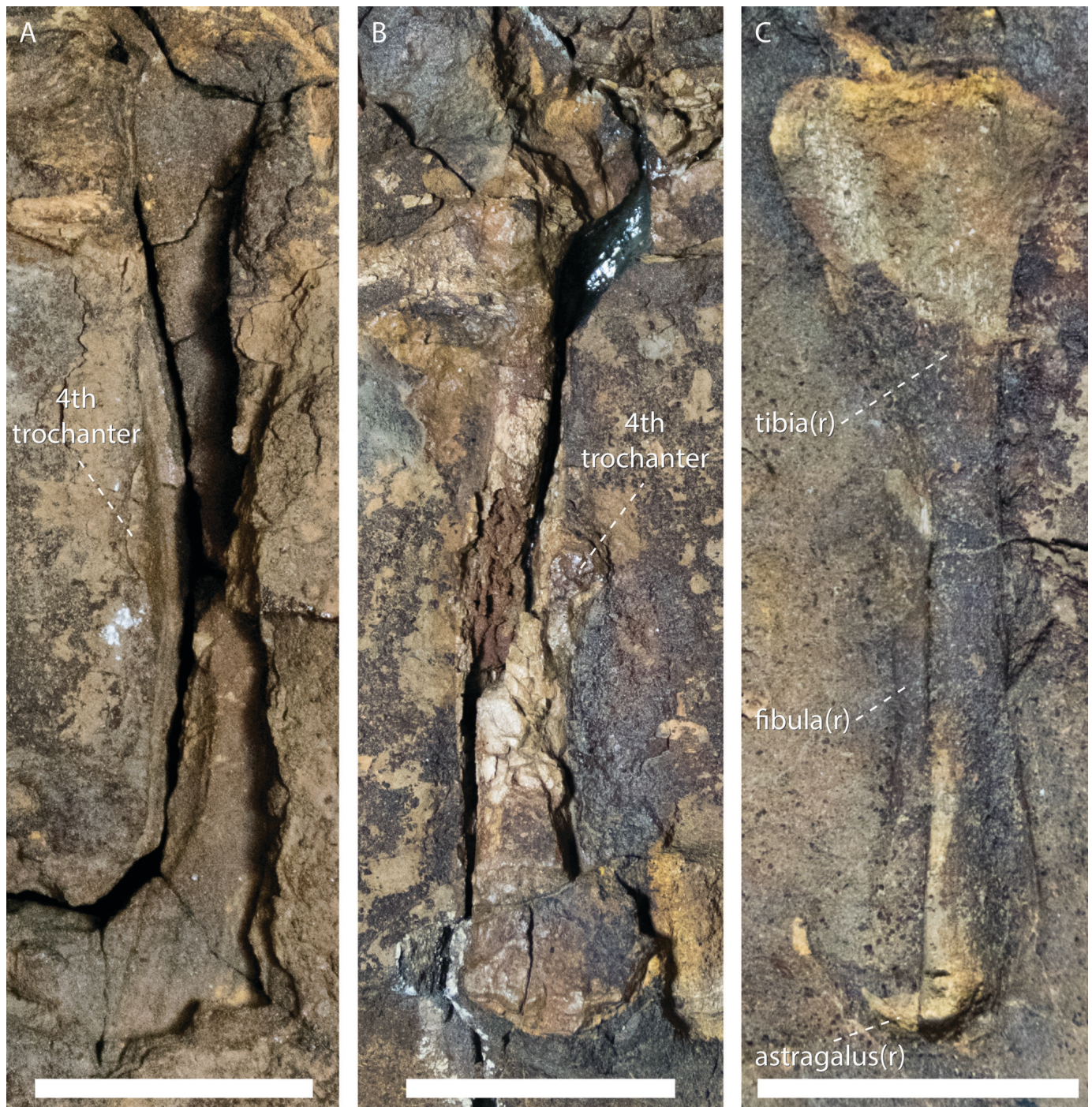


FIGURE 7. Major hind limb elements of UCMP 128181. **A**, left femur from counterpart; **B**, right femur from main block; **C**, right tibia, fibula, and astragalus from main block. Scale bars equal 4 cm.

constriction that terminates in an anterior paddle-like blade and is subellipsoidal and asymmetrical in lateral view (Prieto-Márquez, 2010:character 253 [3, oval expansion, well-pronounced concave profiles along neck]). The shape of the anterior end of the prepubic process varies in Hadrosaurinae and has been used to characterize hadrosaurid genera (Brett-Surman and Wagner, 2007; Prieto-Márquez, 2010). The prepubic process in UCMP 128181 expands more ventrally than dorsally, a morphology that characterizes the

genus *Edmontosaurus* (Prieto-Márquez, 2010:character 252 [1, ventral region is more expanded and directed ventrally]; Prieto-Márquez, 2014). Although none of the autapomorphies of *E. annectens* are present in UCMP 128181 due to the lack of cranial material, we tentatively refer the specimen to this taxon because it is the only *Edmontosaurus* species known from the Hell Creek Formation despite over a century of intense collecting (Campione and Evans, 2011; Horner et al., 2011; Prieto-Márquez, 2014).

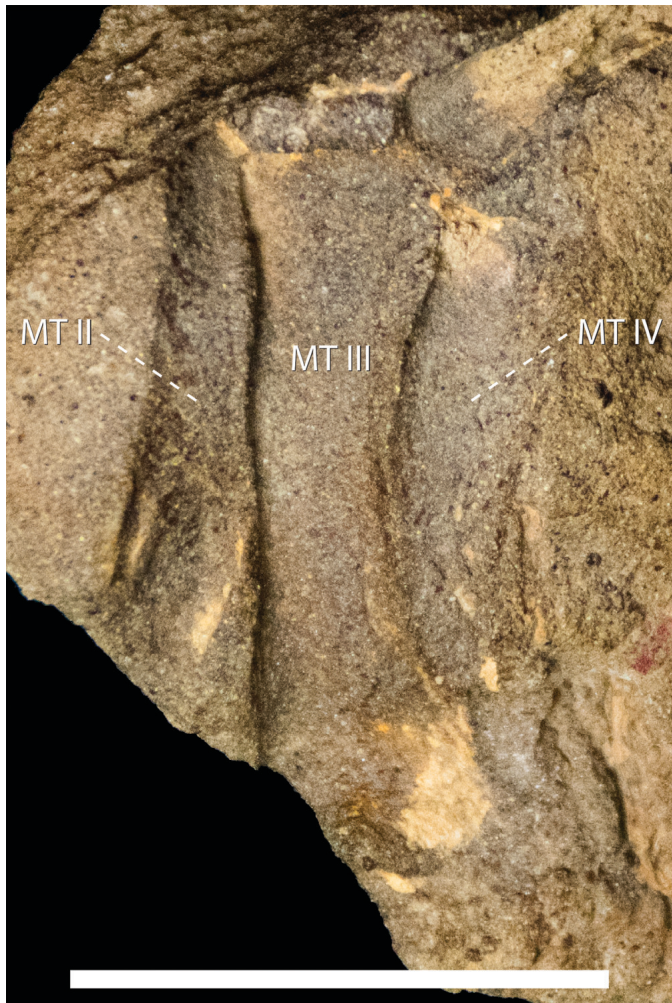


FIGURE 8. Right metatarsals of UCMP 128181 main block. Left-most is metatarsal II. Scale bar equals 4 cm.

RESULTS

Bivariate Analyses

Results of the limb regression analyses are presented in Figure 9 and Tables 3 and 4. Although 25 associated *Edmontosaurus* skeletons were measured, relatively few are completely preserved for all the sampled variables; the most inclusive of the 25 comparisons included 22 specimens (comp. 12: tibia length). At the genus level, 24 out of 25 comparisons are based on 10 or more specimens. At the *E. annectens* species level, 15 out of 25 comparisons are based on 10 or more specimens, whereas comparisons at the *E. regalis* species level have small sample sizes and the lack of juvenile specimens severely limits their potential significance. The size distribution of the specimens is strongly left skewed, making our sample biased towards adults. This constitutes an ‘adult-biased’ sample as defined by Brown and Vavrek (2015), suggesting that the results are vulnerable to type II errors given the small number of data points for each comparison. In general, comparisons pertaining to more distal elements (e.g., radius, metacarpals) had lower sample sizes for both the forelimb and hind limb, which may be directly related to taphonomic modes of preservation. Coefficients of determination (R^2) associated with the regressions using the genus-level data set are generally high (>0.92), although

those associated with the zeugopodial and autopodial elements of the forelimb, where the sample size is smaller, tend to be lower (>0.81).

Forelimb—Fifteen comparisons (comp. 1–10, 20–24 in Tables 3 and 4; Fig. 9A, B, D) describe the growth of the forelimb and were regressed against femur length or the respective element length. At the genus level, two comparisons include the nestling UCMP 128181 (comp. 2: scapular blade height; comp. 3: scapular neck height) and have significant isometric relationships. When the data are subsampled at the genus level by removing the nestling UCMP 128181, the SMA slopes for the forelimb range between 0.926 and 1.300, demonstrating a high degree of isometry in the forelimb as a whole. However, 95% confidence intervals (1.01–1.50) of the SMA slope have a weak positively allometric trend for the ulna (comp. 9), although this weak trend is not reflected in the OLS results. A similar pattern is recovered for the comparison between scapula length and blade height (comp. 20), but this may be affected by incomplete preservation and/or reconstruction of the distal region of the scapular blade in some of the larger specimens. At the *E. annectens* species level, the SMA slopes range between 0.922 and 1.386 and provide isometric relationships except for comparisons related to scapula blade height (comp. 2, 20)—one of two comparisons that include UCMP 128181. For *E. regalis*, only three (comp. 3: scapula neck height; comp. 4: humerus length; comp. 9: ulna length) of the 13 comparisons pass a significance test of $P < 0.05$ and have weakly significant isometric relationships.

Hind Limb—Seven comparisons (comp. 11–15, 19, 25 in Tables 3 and 4; Fig. 9C, D), five of which use femur length as the standard variable, describe the growth of the major components of the hind limb apparatus. At the genus level, three comparisons include UCMP 128181 (comp. 12: tibia length; comp. 14: fibula length; comp. 15: metatarsal III length) and have generally isometric relationships for the zeugopodial elements, whereas metatarsal III has a weakly negative allometric relationship. The slopes are tightly constrained and range between 0.921 and 1.185 (SMA). When the data are subsampled by removing UCMP 128181, the slopes of the three hind limb length comparisons (comp. 12, 14, 15) range between 0.971 and 1.030 (SMA), and the 95% confidence intervals of the SMA slopes indicate isometric trends, including the femur-tibia circumference comparison (comp. 19). At the *E. annectens* species level, all five comparisons have isometric relationships for the complete genus-level data set and when UCMP 128181 is removed. For *E. regalis*, none of five comparisons pass a significance test of $P < 0.05$.

Forelimb versus Hind Limb—Three comparisons (comp. 16–18 in Table 4; Fig. 9E) describe the overall relationship between the forelimb and hind limb apparatuses. Specimen UCMP 128181 does not contribute to these results because the forelimb is not preserved. At the genus level, the comparison of minimum diaphyseal circumference between the humerus and femur (comp. 18) is significantly linear and cannot be distinguished from isometry (slope = 1.025). Notably, the slopes of the SMA regressions are nearly 1.0 (Fig. 9F), which implies isometry between the stylopodial elements. The same relationships are reflected for the *E. annectens* sample, but *E. regalis* does not pass significance tests. When the combined forelimb length (humerus + radius + metacarpal III) is regressed against the combined hind limb length (femur + tibia + metatarsal III), the data have isometric relationships for all subsampled comparisons at the genus and species levels. When this comparison (comp. 16) itself is subsampled by removing the autopodial elements (comp. 17) to increase the sample size, the relationships remain isometric (slope = 1.069), except for the *E. regalis*

TABLE 3. Standard major axis (SMA) results from the bivariate morphometric analyses of appendicular element variables against total femur length (x).

Comparison (y)	Sample	N	Slope (m)	95% CI m	Intercept (b)	95% CI b	R ²	Trend		
1. Scapula length	All – UCMP	17	0.990	0.79	1.24	-0.127	-1.83	1.24	0.835	iso
	<i>E. annectens</i>	12	1.016	0.77	1.33	-0.298	-2.49	1.37	0.848	iso
	<i>E. regalis</i>	5	1.090*	0.48	2.49	-0.864	-10.74	3.45	0.746	iso
2. Scapula blade height	All	16	0.954	0.85	1.07	-1.426	-2.22	-0.71	0.959	iso
	All – UCMP	15	1.243	0.98	1.57	-3.435	-5.69	-1.64	0.846	iso
	<i>E. annectens</i>	12	0.960	0.84	1.09	-1.454	-2.36	-0.66	0.965	iso
	– UCMP	11	1.304	1.01	1.68	-3.834	-6.43	-1.82	0.885	pos
3. Scapula neck height	<i>E. regalis</i>	4	1.364*	0.35	5.26	-4.355	-31.81	2.77	0.651	iso
	All	17	1.094	0.95	1.26	-2.718	-3.87	-1.72	0.932	iso
	All – UCMP	16	1.277	0.91	1.80	-3.992	-7.63	-1.41	0.625	iso
	<i>E. annectens</i>	11	1.123	0.94	1.34	-2.871	-4.33	-1.65	0.944	iso
4. Humerus length	– UCMP	10	1.386	0.88	2.19	-4.687	-10.23	-1.18	0.662	iso
	<i>E. regalis</i>	6	1.505	0.93	2.44	-5.700	-12.31	-1.63	0.868	iso
	All – UCMP	17	1.074	0.94	1.23	-1.115	-2.21	-0.16	0.938	iso
	<i>E. annectens</i>	12	1.090	0.92	1.29	-1.219	-2.61	-0.04	0.941	iso
5. Humerus deltopectoral crest length	<i>E. regalis</i>	5	1.369	0.77	2.42	-3.224	-10.68	0.99	0.892	iso
	All – UCMP	11	0.958	0.73	1.26	-0.930	-3.05	0.68	0.862	iso
	<i>E. annectens</i>	7	0.968	0.66	1.43	-1.004	-4.18	1.15	0.879	iso
	<i>E. regalis</i>	4	0.793*	0.15	4.23	0.237	-24.05	4.79	0.283	iso
6. Humerus deltopectoral crest width	All – UCMP	10	1.141	0.96	1.36	-3.013	-4.55	-1.73	0.953	iso
	<i>E. annectens</i>	6	1.036	0.79	1.36	-2.310	-4.55	-0.61	0.960	iso
	<i>E. regalis</i>	4	1.104*	0.42	2.93	-2.713	-15.67	2.18	0.860	iso
	All – UCMP	14	1.231	0.96	1.58	-3.125	-5.52	-1.25	0.842	iso
7. Humerus circumference	<i>E. annectens</i>	11	1.283	0.94	1.75	-3.470	-6.66	-1.12	0.828	iso
	<i>E. regalis</i>	3	1.803*	0.61	5.32	-7.234	-32.19	1.23	0.989	iso
	All – UCMP	14	1.135	0.92	1.40	-1.618	-3.46	-0.12	0.888	iso
	<i>E. annectens</i>	9	1.069	0.82	1.39	-1.179	-3.42	0.54	0.910	iso
8. Radius length	<i>E. regalis</i>	5	0.704*	0.24	2.09	1.472	-8.35	4.77	0.485	iso
	All – UCMP	15	1.229	1.01	1.50	-2.160	-4.03	-0.63	0.890	pos
	<i>E. annectens</i>	10	1.120	0.87	1.45	-1.435	-3.68	0.30	0.900	iso
	<i>E. regalis</i>	5	0.942	0.44	2.03	-0.082	-7.78	3.49	0.788	iso
10. Metacarpal III length	All – UCMP	11	1.017	0.73	1.45	-1.530	-4.51	0.56	0.773	iso
	<i>E. annectens</i>	7	1.049	0.64	1.72	-1.723	-6.33	1.09	0.800	iso
	<i>E. regalis</i>	4	1.529*	0.42	5.55	-5.197	-33.61	2.63	0.696	iso
	All	18	1.025	0.92	1.14	-1.081	-1.84	-0.39	0.962	iso
11. Femur circumference	All – UCMP	17	1.194	0.93	1.53	-2.252	-4.56	-0.45	0.795	iso
	<i>E. annectens</i>	14	1.034	0.93	1.15	-1.131	-1.88	-0.46	0.973	iso
	– UCMP	13	1.257	0.98	1.61	-2.667	-5.11	-0.76	0.857	iso
	<i>E. regalis</i>	4	1.329*	0.26	6.81	-3.270	-41.93	4.28	0.344	iso
12. Tibia length	All	22	0.985	0.93	1.04	-0.022	-0.40	0.33	0.987	iso
	– UCMP	21	1.030	0.89	1.19	-0.336	-1.42	0.60	0.914	iso
	<i>E. annectens</i>	16	0.980	0.93	1.03	0.007	-0.32	0.32	0.993	iso
	All – UCMP	15	1.014	0.88	1.17	-0.226	-1.30	0.70	0.943	iso
13. Tibia circumference	<i>E. regalis</i>	6	1.122*	0.51	2.45	-0.982	-10.36	3.31	0.612	iso
	All – UCMP	13	1.157	0.98	1.36	-2.232	-3.66	-1.02	0.938	iso
	<i>E. annectens</i>	9	1.154	0.90	1.48	-2.207	-4.43	-0.47	0.922	iso
	<i>E. regalis</i>	4	1.376*	1.17	1.62	-3.789	-5.53	-2.31	0.997	pos
14. Fibula length	All	20	1.030	0.98	1.09	-0.405	-0.79	0.04	0.988	iso
	All – UCMP	19	0.971	0.84	1.13	0.005	-1.09	0.95	0.913	iso
	<i>E. annectens</i>	15	1.033	0.98	1.09	-0.424	-0.83	-0.04	0.991	iso
	– UCMP	14	0.982	0.83	1.16	-0.071	-1.33	0.99	0.926	iso
15. Metatarsal III length	<i>E. regalis</i>	5	0.864*	0.36	2.06	0.764	-7.61	4.28	0.716	iso
	All	13	0.921	0.85	1.00	-0.577	-1.10	-0.09	0.985	neg
	All – UCMP	12	0.986	0.79	1.23	-1.028	-2.72	0.33	0.900	iso
	<i>E. annectens</i>	8	0.924	0.83	1.03	-0.597	-1.33	0.06	0.987	iso
Estimation of Forelimb Lengths and Body Mass in UCMP 128181	– UCMP	7	1.028	0.73	1.44	-1.312	-4.15	0.71	0.910	iso
	<i>E. regalis</i>	5	0.732*	0.31	1.74	0.753	-6.37	3.74	0.714	iso

Regression formulas expressed as $\ln(y) = m \cdot \ln(x) + b$. Positive or negative allometry is considered to be demonstrated when the slopes of the lines are significantly different from a slope of 1, as indicated by the 95% confidence intervals.

*No significant correlation between variables (two-tailed t test; $P > 0.05$).

species level, which results in a weakly negative allometric relationship.

Estimation of Forelimb Lengths and Body Mass in UCMP 128181

Ordinary least squares regression of the genus-level data set was used to predict missing data for UCMP 128181, with particular reference to the forelimb comparisons (Table 5). With respect to the total length of the forelimb

(humerus [comp. 4] + radius [comp. 8] + metacarpal III [comp. 10]), a notable discrepancy of 9 mm occurs between the sum of individual limb element estimates (184.9 mm) and when they are considered in concert as a single variable (comp. 16; 193.9 mm). A similar discrepancy occurs for the humerus + radius variable (comp. 17) between the OLS-predicted value (149.4 mm) and the summative value (140.6 mm). Therefore, we predict that the total length of the forelimb for UCMP 128181 is between 185 and

TABLE 4. Standard major axis (SMA) results from the bivariate morphometric analyses of circumference, combined limb length, and intrabone comparisons.

Comparison (x: y)	Sample	N	Slope (m)	95% CI m	Intercept (b)	95% CI b	R ²	Trend
16. Hind limb length: Forelimb length	All – UCMP	9	1.048	0.86 – 1.28	-0.894	-2.66 – 0.56	0.951	iso
	<i>E. annectens</i>	5	1.046	0.67 – 1.64	-0.883	-5.41 – 2.01	0.936	iso
	<i>E. regalis</i>	4	0.959	0.57 – 1.62	-0.194	-5.34 – 2.86	0.968	iso
17. Femur+tibia lengths: Humerus+radius lengths	All – UCMP	13	1.069	0.91 – 1.25	-1.092	-2.50 – 0.11	0.941	iso
	<i>E. annectens</i>	8	1.065	0.81 – 1.40	-1.069	-3.58 – 0.84	0.923	iso
	<i>E. regalis</i>	5	0.882	0.83 – 0.93	0.350	-0.05 – 0.72	0.999	neg
18. Femur circumference: Humerus circumference	All – UCMP	14	1.025	0.80 – 1.31	-0.754	-2.44 – 0.57	0.849	iso
	<i>E. annectens</i>	11	1.019	0.79 – 1.32	-0.735	-2.55 – 0.66	0.879	iso
	<i>E. regalis</i>	3	0.599*	0.04 – 9.13	1.911	-50.32 – 5.34	0.643	iso
19. Femur circumference: Tibia circumference	All – UCMP	14	1.008	0.77 – 1.32	-0.268	-2.14 – 1.16	0.813	iso
	<i>E. annectens</i>	10	0.974	0.73 – 1.30	-0.074	-2.00 – 1.37	0.873	iso
	<i>E. regalis</i>	4	1.035*	0.20 – 5.31	-0.404	-26.48 – 4.68	0.343	iso
20. Scapula length: Scapula blade height	All – UCMP	15	1.286	1.04 – 1.60	-3.486	-5.57 – 1.81	0.869	pos
	<i>E. annectens</i>	11	1.306	1.04 – 1.63	-3.599	-5.80 – 1.84	0.910	pos
	<i>E. regalis</i>	4	1.943*	0.48 – 7.93	-8.032	-49.02 – 2.01	0.602	iso
21. Scapula length: Scapula neck height	All – UCMP	17	1.300	0.92 – 1.84	-3.900	-7.51 – 1.35	0.591	iso
	<i>E. annectens</i>	12	1.339	0.86 – 2.08	-4.137	-9.08 – 0.95	0.587	iso
	<i>E. regalis</i>	5	1.312*	0.59 – 2.92	-4.050	-14.95 – 0.86	0.768	iso
22. Humerus length: Humerus circumference	All – UCMP	16	1.189	0.94 – 1.51	-2.094	-4.14 – 0.48	0.821	iso
	<i>E. annectens</i>	13	1.227	0.93 – 1.62	-2.324	-4.79 – 0.45	0.821	iso
	<i>E. regalis</i>	3	1.811*	0.11 – 29.60	-6.188	-186.65 – 4.86	0.590	iso
23. Humerus length: Humerus deltopectoral crest length	All – UCMP	12	0.926	0.71 – 1.20	-0.144	-1.91 – 1.21	0.857	iso
	<i>E. annectens</i>	8	0.922	0.65 – 1.30	-0.128	-2.52 – 1.56	0.876	iso
	<i>E. regalis</i>	4	0.616*	0.14 – 2.70	1.870	-11.55 – 4.93	0.533	iso
24. Humerus length: Humerus deltopectoral crest width	All – UCMP	12	1.126	0.99 – 1.28	-2.213	-3.16 – 1.37	0.969	iso
	<i>E. annectens</i>	8	1.080	0.88 – 1.25	-1.936	-3.01 – 0.55	0.970	iso
	<i>E. regalis</i>	4	0.998*	0.28 – 3.58	-1.356	-18.17 – 3.33	0.704	iso
11. Femur length: Femur circumference	All	18	1.025	0.92 – 1.14	-1.081	-1.84 – 0.39	0.962	iso
	All – UCMP	17	1.194	0.93 – 1.53	-2.252	-4.56 – 0.45	0.795	iso
	<i>E. annectens</i>	14	1.034	0.93 – 1.15	-1.131	-1.88 – 0.46	0.973	iso
25. Tibia length: Tibia circumference	– UCMP	13	1.257	0.98 – 1.61	-2.667	-5.11 – 0.76	0.857	iso
	<i>E. regalis</i>	4	1.329*	0.26 – 6.81	-3.270	-41.93 – 4.28	0.344	iso
	All – UCMP	15	1.185	0.97 – 1.44	-2.256	-4.00 – 0.83	0.892	iso
	<i>E. annectens</i>	11	1.197	0.99 – 1.45	-2.329	-4.02 – 0.93	0.936	iso
	<i>E. regalis</i>	4	1.423*	0.31 – 6.50	-3.923	-39.06 – 3.76	0.488	iso

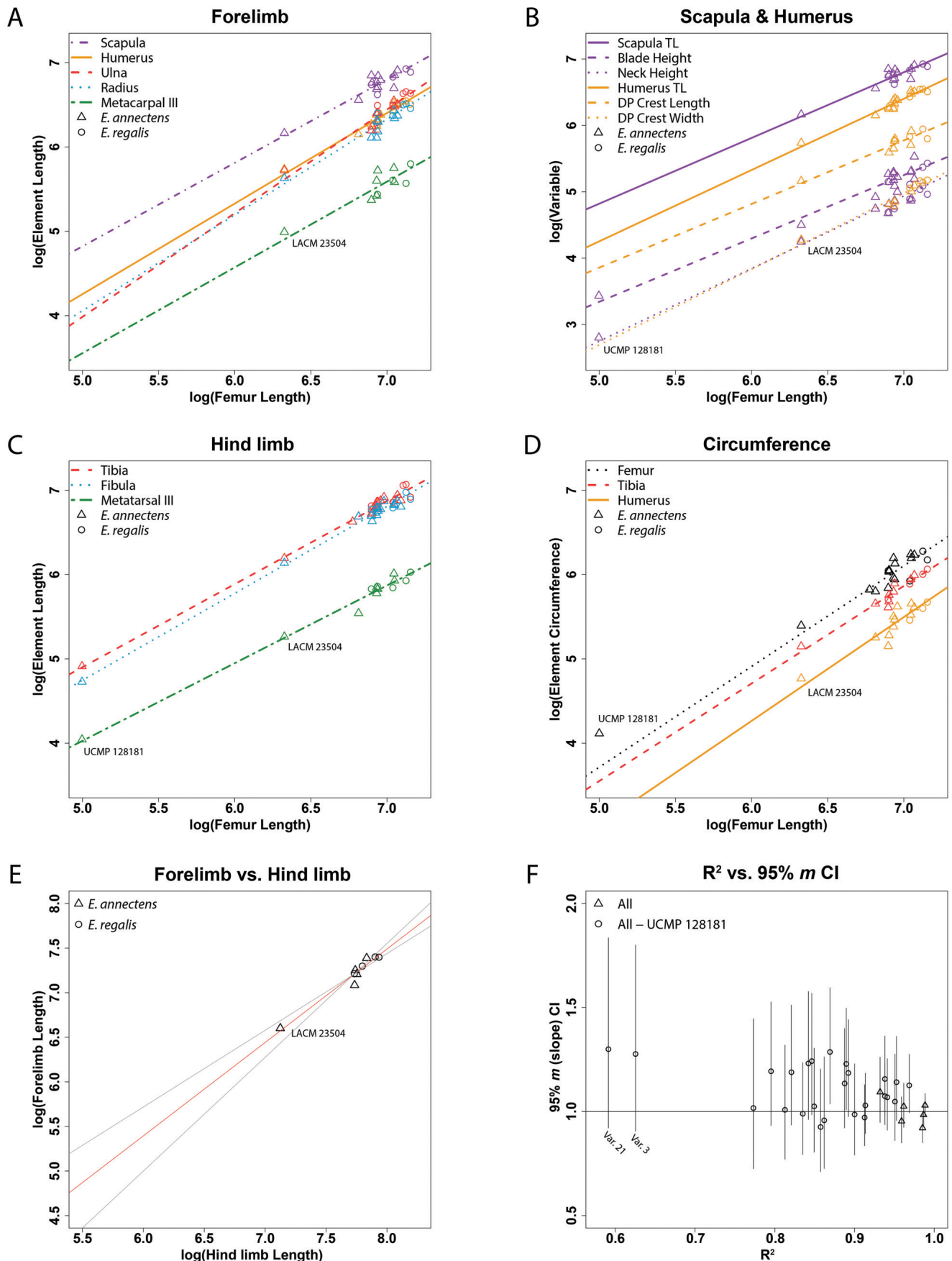
Regression formulas expressed as $\ln(y) = m \cdot \ln(x) + b$. Positive or negative allometry is considered to be demonstrated when the slopes of the lines are significantly different from a slope of 1, as indicated by the 95% confidence intervals.

*No significant correlation between variables (two-tailed t test; $P > 0.05$).

TABLE 5. Estimated OLS regression values for UCMP 128181 from comparisons using femur length as the standard variable (Supplementary Data 1, Table S2).

Element	Dimension	UCMP 128181	All		Edmontosaurus UCMP 128181		<i>E. annectens</i> UCMP 128181	
			OLS	% Error	OLS	% Error	OLS	% Error
Scapula	Total length	—	—	—	146.10	—	138.98	—
	Blade height	31	29.29	5.85%	19.44	59.45%	16.92	83.24%
	Neck height	16.5	16.71	-1.28%	18.30	-9.83%	15.28	7.97%
Humerus	Total length	—	—	—	75.00	—	73.03	—
	Deltpectoral crest length	—	—	—	47.34	—	46.21	—
	Deltpectoral crest width	—	—	—	15.57	—	18.25	—
Radius	Minimum circumference	—	—	—	25.19	—	23.66	—
	Total length	—	—	—	65.63	—	70.47	—
	Ulna	—	—	—	61.47	—	71.75	—
Metacarpal III	Total length	—	—	—	44.30	—	41.62	—
	Femur	148	—	—	—	—	—	—
	Minimum circumference	60	58.99	1.71%	52.56	14.16%	44.24	35.62%
Tibia	Total length	136	135.74	0.19%	134.10	1.42%	133.68	1.73%
	Minimum circumference	—	—	—	37.28	—	38.27	—
	Fibula	113	116.11	-2.68%	140.31	-19.46%	135.51	-16.61%
Metatarsal III	Total length	57	56.68	0.56%	54.39	4.81%	45.80	24.45%

Percent error was calculated using a ratio of the actual UCMP 128181 measurement and the OLS-estimated value.



194 mm, with a 5% error range among different manipulations of the data set.

Body mass of UCMP 128181 was estimated using the length (148 mm) and estimated circumference (60 mm) of the right femur. When using the adult-sized CCM *E. annectens* skeleton as a comparative standard (body mass estimate = 6922 ± 1772 kg via equation 1 of Campione and Evans, 2012) for developmental mass extrapolation, UCMP 128181 was estimated to have weighed 14.7 kg based on femur length and 12.7 kg based on femur circumference.

DISCUSSION

The UCMP 128181 skeleton is the youngest known ontogeny morph of *Edmontosaurus* (Campione and Evans, 2011) and one of the smallest nonembryonic hadrosaurid skeletons on record, with a femur length of 148 mm and an estimated body mass of 14 kg. For comparison, previously reported hadrosaurid egg volumes (Horner, 1999) were converted using an average bird egg content density of 1.031 kg/m³ (Rahn et al., 1982). This provided approximate body mass estimates of 1–4 kg for freshly hatched hadrosaurids, whereas body mass estimates for the previously smallest *Edmontosaurus* juvenile LACM 23504 skeleton are approximately 791 kg (femur length) and 627 kg (femur circumference). Horner et al. (2000) defined ontogenetic growth stages in *Maiasaura* based on osteohistological criteria, body size, and egg, nest, and adult associations, a system that has been extended to other hadrosaurids (Table 6). The categorization used for *Maiasaura* identified two stages of nestlings: ‘early nestling,’ with a femur length of 70 mm and a ~450 mm body length, and ‘late nestling,’ with a femur length of 120 mm and a ~900 mm body length (Horner et al., 2000). Embryos attributed to the lambeosaurine *Hypacrosaurus* have a femur that reaches approximately 80 mm in total length, and nestlings of this taxon exceeded the body size of *Maiasaura* late nestlings by almost double. This suggests that lambeosaurines were larger at hatching than hadrosaurines and is consistent with the known difference in egg sizes between these two taxa (Horner, 1999). Additionally, Barsbold and Perle (1983) reported on the remains of baby hadrosaurs with femur lengths of 40–50 mm associated with nesting sites from the Tugrik Shire locality of Mongolia, and recent finds of partially articulated *Sauropelodus* specimens associated with egg-shells from the Nemegt Formation of Mongolia were identified as embryos with a femur length of 43.5 mm (Dewaele et al., 2015).

The femur length of UCMP 128181 is slightly greater than in late nestlings of *Maiasaura* but is significantly shorter than in nestlings of *Hypacrosaurus*. *Edmontosaurus* adults attain a larger body size than *Maiasaura*. Therefore, we predict that *Edmontosaurus* neonates were slightly larger than *Maiasaura* neonates at hatching and attained a larger size during the nestling stage. For these reasons, we assign UCMP 128181 to the late nestling stage of Horner et al. (2000). Perinatal dinosaur material is very rare in the Hell Creek Formation and its equivalents (Russell and Manabe, 2002; Horner et al., 2011), and to our knowledge, UCMP 128181 represents the only nestling dinosaur skeleton from the Hell Creek Formation and late Maastrichtian deposits of the Western Interior. Carpenter (1982) described a partial left dentary (UCM 41666) and basioccipital (UCM 43218) and referred them to *Sauornithoides* (= *Troodon*) *inequalis*, along with a collection of small teeth, some of which belonged to

TABLE 6. Total femur length measurements (mm) of hadrosaurid ontogenetic stages.

Taxon	Size class	Specimen no.	Femur (mm)
<i>Edmontosaurus</i>	Early nestling	—	—
	Late nestling	UCMP 128181	148
	Early juvenile	—	—
	Late juvenile	LACM 23504	567
	Subadult	CNMH 10178	910
	Adult	AMNH 5730	1148
<i>Hypacrosaurus</i> ¹	Embryonic	MOR 562	80
	Nestling	MOR 548	168–235
	Juvenile	MOR 35	600
	Subadult	MOR 553	870
	Adult	MOR 549	1050
<i>Maiasaura</i> ²	Early nestling	YPM-PU 22432	70
	Late nestling	YPM-PU 22400	120
	Early juvenile	YPM-PU 22472	180
	Late juvenile	MOR-005JV	500
	Subadult	MOR-005SA	680
<i>Sauropelodus</i>	Adult	MOR-005A	1000
	Embryonic ³	MPC-D100/764	43.5
	Adult ⁴	PIN 551-8	1200

Ontogenetic stages as defined by Horner et al. (2000), unless otherwise noted by an additional citation for which the original categorization was followed. Data were collected by the authors first hand and from published literature.

¹Horner and Currie, 1994; ²Horner et al., 2000; ³Dewaele et al., 2015;

⁴Maryńska and Osmolska, 1984.

presumed hatchling hadrosaurids (UCM 45060, UCM 45061). Although this material originated from the contiguous Lance Formation (UCM locality 77067 ‘Bushy Tailed Blowout’; also UCMP locality V5711), it represented the only documented evidence for hatchling dinosaur material from the late Maastrichtian of the Western Interior Basin. Goodwin et al. (2006) described a relatively complete skull of the smallest and ontogenetically youngest *Triceratops* (UCMP 154452) and later inferred the previous lack of ontogenetically younger *Triceratops* from the Hell Creek Formation to be, in part, a product of historical collection bias aimed in favor of larger and better identifiable fossils preserved in sandstones in the field, with little or no attention to mudstone deposits (Goodwin and Horner, 2014). However, limitations on the abundance of juvenile specimens may also be related to strong taphonomic biases against the preservation of small-bodied skeletons in fluvial systems (Brown et al., 2013a, 2013b).

Limb Allometry of *Edmontosaurus* and Gait Change in Hadrosaurs

Studies of relative cranial growth in hadrosaurid dinosaurs have documented extreme changes through ontogeny with the development of large cranial crests that greatly impacted our view of their taxonomy and biology (e.g., Dodson, 1975; Evans, 2010; Campione and Evans, 2011; McGarritty et al., 2013; Freedman Fowler and Horner, 2015). Compared with the skull, the ontogeny of the postcranial skeleton has not been studied intensely and only a few investigations of ontogenetic allometry have been conducted to date (Dilkes, 2001; Guenther, 2009, 2014; Kilbourne and Makovicky, 2010; Farke et al., 2013). Dilkes (2001) used multivariate and bivariate morphometrics and the

← FIGURE 9. Bivariate allometric results. SMA regressions for a variety of appendicular measurements against femur length (**A–D**) or combined hind limb length (**E**). **A**, total lengths of forelimb elements; **B**, scapular and humeral variables; **C**, total lengths of hind limb elements; **D**, minimum diaphyseal circumferences using the ‘All – UCMP’ samples to maintain consistency, estimated UCMP 128181 value from digital cross-section was included in figure for visual comparison only; **E**, combined forelimb versus hind limb lengths, with 95% confidence intervals; **F**, overall results of most inclusive SMA regression analyses, symbol corresponds with slope (m) and vertical bars correspond with the upper and lower bounds of 95% confidence intervals (CIs) of the slope (m). SMA statistics are presented in Tables 3 and 4.

biomechanics of beam theory on a growth series of disassociated elements of *Maiasaura peeblesorum* and proposed a major gait shift from biped juveniles to quadrupedal adults in this taxon. This pattern was subsequently generalized among hadrosaurs (Horner et al., 2004). Herein, gait refers to the natural pattern of movement of the limbs during the animal's predominant form of locomotion. This study of *Edmontosaurus* does not address cortical bone thickness or internal cross-sectional properties of the limb bones, which were critical in the formulation of the ontogenetic gait shift hypothesis of Dilkes (2001). However, the ontogenetic analysis of limb proportions does provide the fundamental components of data for assessing this idea. Because few articulated skeletons are available for *Maiasaura*, metrics associated with ontogenetic changes in limb proportions within the skeleton (e.g., forelimb vs. hind limb) used to hypothesize ontogenetic gait changes in other dinosaurs (e.g., Reisz et al., 2005; Zhao et al., 2013) could not be calculated for this taxon. The relative lengths and robustness of limbs have long been noted to differ between clades of hadrosaurids (Brett-Surman and Wagner, 2007; Guenther, 2009), suggesting possible variability in hadrosaur locomotor dynamics. However, the ontogenetic gait shift hypothesis has not been investigated in any other hadrosaurid taxon despite an abundance of available material from numerous taxa. For *Edmontosaurus*, the ontogenetic gait shift hypothesis can be corroborated if the forelimbs are relatively shorter than the hind limbs in juveniles and exhibit positive allometry through growth. This prediction is based on the hypothesis of Dilkes (2001), in which juvenile hadrosaurs were primarily bipeds and shifted towards a quadrupedal stance with maturity and the drastic limb scaling trends in other dinosaurian taxa with hypothesized gait shifts (Reisz et al., 2005; Zhao et al., 2013).

Bivariate regression analyses based on articulated skeletons indicate a largely isometric relationship throughout the ontogeny of the postcranial limb skeleton in *Edmontosaurus* when analyzed at the genus and *E. annectens* species levels. The majority of comparisons at the *E. regalis* species level fail significance tests of correlation between variables, which can be attributed to a limited size range and small sample sizes, and are not further discussed. At the genus level, the lengths of the forelimb elements, for which UCMP 128181 cannot be analyzed due to a lack of preservation, have near-isometric relationships through ontogeny with the exception of ulna length (comp. 9), which exhibits very weak positive allometry (genus: $R^2 = 0.89$, 95% confidence interval [CI] of the slope [m] = 1.01–1.50), which is probably due to the elongation of the olecranon process (Maidment and Barrett, 2014). However, at the *E. annectens* species level, growth of the ulna relative to the femur cannot be distinguished from isometry. The lengths and circumferences of the hind limb elements (comp. 10–14, 25) reflect an even more tightly constrained, isometric relationship, with the exception of the weak negatively allometric metatarsal III length (comp. 15). At the genus and *E. annectens* species levels, the analyses comparing the overall forelimb length with the hind limb length (comp. 16–17) and the minimum diaphyseal circumference of the humerus and femur (comp. 18) exhibit isometry. Similar isometric trends in the limbs occur when the nestling UCMP 128181 specimen is excluded from the analyses, indicating that UCMP 128181 is not strongly influencing the allometric results.

Dilkes (2001) observed weak negative allometry in intrabone length and circumference regressions in *Maiasaura peeblesorum* for the humerus (RMA slope = 0.96), femur (RMA slope = 0.95), and tibia (RMA slope = 0.97) suggesting a slight ontogenetic decrease in the robustness of these limbs through growth. Kilbourne and Makovicky (2010) also observed an ontogenetic decrease in robustness in equivalent intrabone comparisons of *Maiasaura* and *Hypacrosaurus*. The *Edmontosaurus* data presented here (comp. 11, 22, 25) differ from both of these studies in that the slopes of the intrabone length to circumference in the humerus (1.19), femur (1.03), and tibia (1.19) trend slightly

positive, but all are considered here to be isometric due to larger confidence intervals (Table 4). It is important to note that even though our sample sizes are occasionally limited, high R^2 values (0.82 [humerus]; 0.89 [tibia]; 0.96 [femur]) and constrained confidence intervals of slopes indicate concordant trends of weak positive allometry in the robustness of all three of these major limb bones through ontogeny. Beyond hadrosaurids, obligate quadrupedal dinosaurs such as sauropods, stegosaurs, and ceratopsids (Kilbourne and Makovicky, 2010) as well as the modern *Alligator mississippiensis* (Livingston et al., 2009) exhibit largely isometric trends in the robustness of their limbs through ontogeny, with only a few notable exceptions (e.g., *Agujaceratops*, femur). Differences between *Maiasaura*, *Hypacrosaurus*, and *Edmontosaurus* may be taxon specific and reflect different life history strategies in locomotor dynamics, suggesting that care should be taken when extrapolating interpretations to larger clades.

The absence of the forelimb of UCMP 128181 is not optimal for testing the gait shift hypothesis early in ontogeny. However, its length can be estimated based on the remainder of the sample to compare with other associated individuals as an external test of the feasibility of the recovered limb relationships. We estimate that the missing forelimb of UCMP 128181 was between 54% and 57% of the total hind limb length (341 mm). This is comparable to the measured ratio in the only known *Edmontosaurus* juvenile specimen LACM 23504 (59%) but is generally on the low end compared with the range of variation in presumably adult specimens of *E. annectens* in our data set (52% [USNM 2414], 58% [SDSM 4917], 62% [YPM-PU 2182], and 64% [AMNH 5730]). *Hypacrosaurus* perinates (52% [MOR 548]; Horner and Currie, 1994) and nestlings (65% [ROM 53594]) fall within the range of variation for *Edmontosaurus*, whereas *Sauropelodus* perinates exhibit a slightly larger forelimb–hind limb ratio (69% [MPC-D100/764]; Dewaele et al., 2015), further suggesting the potential for quadrupedality at hatching based on limb length proportions. It is important to keep in mind that the estimated length of the UCMP 128181 forelimb, as with hatchlings of other taxa, may underrepresent the total relative forelimb length because of extensive cartilage caps at the epiphyses of limb bones in perinates of this size (Horner and Currie, 1994). This estimate is also based on the forelimb–hind limb relationships of ontogenetically larger and more osteologically mature individuals that likely had relatively smaller cartilage caps (e.g., Bonnan et al., 2010; Holliday et al., 2010).

The appendicular skeleton of hadrosaurids increases in length by an order of magnitude or more during growth (Table 6). Our analysis of *Edmontosaurus* encompasses a broad ontogenetic range with a femur length range of 148–1242 mm and body mass range of 14–6922 kg. This is comparable to the virtually complete growth series known for *Maiasaura* (Horner et al., 2000; Woodward et al., 2015) and *Hypacrosaurus* (Horner and Currie, 1994). Overall, the relative growth of the limbs across this wide ontogenetic spectrum varies marginally from isometry and does not necessitate a gait shift as the differences in limb proportions dictate in other nonavian dinosaur taxa such as *Psittacosaurus* (Zhao et al., 2013) and *Massospondylus* (Reisz et al., 2005). The relative length of the forelimb to the hind limb is maintained from juveniles (LACM 23504) to adults, and we can predict a similar ratio in nestlings. Likewise, the relationships between the minimum diaphyseal circumferences of the humerus and femur are also maintained through ontogeny, at least from the juvenile stage, which differs from the predictions of Dilkes (2001). The weak positively allometric trend observed in the ulna (comp. 9) is likely a result of the ontogenetic lengthening of the olecranon process, which has been shown to be characteristic of quadrupedality in ornithischian dinosaurs (Maidment and Barrett, 2014). This may provide some support for an ontogenetic shift towards quadrupedality. However, it may also be a response to posterior shifts in the distribution of mass across the body with growth, rather than accommodating a permanent gait shift. To further test this

hypothesis, it would be beneficial to incorporate variables from the pelvic girdle and other regions of the skeleton, but the poor preservation of these elements across the entire data set makes it difficult to do so. However, the current data illustrate that nestlings were anatomically capable of fully quadrupedal locomotion and provide no compelling evidence to support an ontogenetic gait shift in *Edmontosaurus*. Results from these analyses are consistent with trackway evidence for juvenile hadrosaurids from Denali National Park, Alaska (Fiorillo and Tykoski, 2016). The estimated size of the smallest individuals (~165 cm total body length) that were definitively walking in a quadrupedal gait was intermediate between UCMP 128181 and LACM 23504 (Fiorillo and Tykoski, 2016), suggesting that even at nestling size, hadrosaurids engaged in quadrupedal locomotion.

CONCLUSION

Specimen UCMP 128181 is the first occurrence of a baby dinosaur skeleton from the intensely sampled Hell Creek Formation and greatly expands the known ontogenetic range for *Edmontosaurus* as the smallest end member. Using the previously established categorization of hadrosaurid growth stages (Horner et al., 2000), UCMP 128181 represents a late nestling. Across *Edmontosaurus* ontogeny, bivariate morphometric comparisons reveal that the tested forelimb and hind limb elements exhibit a predominantly isometric growth pattern, especially in the hind limb. This indicates that *Edmontosaurus* was capable of quadrupedal locomotion from the time of hatching. Bipedality was the primitive condition in dinosaurs, but quadrupedality evolved secondarily and independently in many dinosaur groups (Maidment and Barrett, 2014). Studying this major gait shift is essential because it can help assess the evolutionary origin and requirements of quadrupedality. In addition, ontogenetic shifts in gait are interesting because they are highly unusual among terrestrial vertebrates. Future studies will incorporate osteohistology and biomechanics to supplement these allometric analyses and further test the proposed gait shift hypothesis in hadrosaurs.

ACKNOWLEDGMENTS

Access to specimens was facilitated by N. Carroll, M. Currie, P. Holroyd, M. Goodwin, C. Mehling, D. Pagnac, K. Seymour, and K. Shepherd. Our thanks to many across the globe who helped gather measurements and confirm locality information: D. Brinkman, N. Campione, R. Carr, N. Carroll, J. Eberle, J. Mallon, A. Mann, A. McGee, B. Roach, J. Scannella, V. Schneider, H. Seyler, T. Sonoda, and M. Whitney. Comments from R. Butler, A. Farke, D. McLennan, P. O'Connor, and an anonymous reviewer greatly improved the manuscript. We thank C. A. Masnaghetti (artist) and N. Turinetti from Saurian and Urvogel Games, LLC for working with us to design cover art associated with this article. We thank the Twitchell family for their long-term support of field work by the UCMP and crews on and around their ranch. D. Melton and G. Liggett of the Bureau of Land Management Office facilitated access to land under their management. We thank the M. Thomas family who supported Harley in the field during the collection of UCMP 128181. And most importantly, we thank the late H. Garbani, a long-term field associate and friend of the UCMP, who passed away in 2011. The nestling skeleton described in this paper is but one of a number of significant discoveries by Harley and his keen eyes and passion for hunting dinosaur bones over four decades working with W. Clemens and UCMP field crews.

FUNDING

This work was supported by the University of California Museum of Paleontology Doris O. and Samuel P. Welles Research Fund to (to M.W.), a Natural Sciences and

Engineering Research Council of Canada Discovery Grant RGPIN 355845 (to D.C.E.), a Royal Ontario Museum Department of Natural History Fieldwork Grant (to D.C.E.), N. Myrvold in support of the Hell Creek Project III (to M.B.G.), and the University of California Museum of Paleontology (to M.B. G.).

LITERATURE CITED

- Barsbold, R., and A. Perle. 1983. On the taphonomy of group burial of baby dinosaurs and some problems of their ecology. Transactions of the Joint Soviet-Mongolian Paleontological Expedition 24:121–125. [Russian]
- Bonnan, M. F., J. L. Sandrik, T. Nishiwaki, D. R. Wilhite, R. M. Elsey, and C. Vittore. 2010. Calcified cartilage shape in archosaur long bones reflects overlying joint shape in stress-bearing elements: implications for nonavian dinosaur locomotion. The Anatomical Record 293:2044–2055.
- Brett-Surman, M. K., and J. R. Wagner. 2007. Discussion of character analysis of the appendicular anatomy in Campanian and Maastrichtian North American hadrosaurids: variation and ontogeny; pp. 135–169 in K. Carpenter (ed.), Horns and Beaks: Ceratopsians and Ornithopod Dinosaurs. Indiana University Press, Bloomington, Indiana.
- Brown, B. 1907. The Hell Creek beds of the Upper Cretaceous of Montana. Bulletin of the American Museum of Natural History 23:823–845.
- Brown, C. M., and M. J. Vavrek. 2015. Small sample sizes in the study of ontogenetic allometry: Implications for palaeobiology. PeerJ 3:e818.
- Brown, C. M., N. E. Campione, and D. C. Evans. 2013a. Body size related taphonomic biases in the latest Maastrichtian: implications for the end-Cretaceous extinction. Journal of Vertebrate Paleontology 33 (Programs and Abstracts):95.
- Brown, C. M., D. C. Evans, N. E. Campione, L. J. O'Brien, and D. A. Eberth. 2013b. Evidence for taphonomic size bias in the Dinosaur Park Formation (Campanian, Alberta), a model Mesozoic terrestrial alluvial-paralic system. Palaeogeography, Palaeoclimatology, Palaeoecology 372:108–122.
- Campione, N. E. 2014. Postcranial anatomy of *Edmontosaurus regalis* (Hadrosauridae) from the Horseshoe Canyon Formation, Alberta, Canada; pp. 208–244 in D. A. Eberth and D. C. Evans (eds.), Hadrosaurs. Indiana University Press, Bloomington, Indiana.
- Campione, N. E., and D. C. Evans. 2011. Cranial growth and variation in edmontosaurs (Dinosauria: Hadrosauridae): implications for latest Cretaceous megaherbivore diversity in North America. PLoS ONE 6: e25186.
- Campione, N. E., and D. C. Evans. 2012. A universal scaling relationship between body mass and proximal limb bone dimensions in quadrupedal terrestrial tetrapods. BMC Biology 10:60.
- Carpenter, K. 1982. Baby dinosaurs from the Late Cretaceous Lance and Hell Creek formations and a description of a new species of theropod. Contributions to Geology 20:123–134.
- Christians, J. P. 1992. Taphonomy and sedimentology of the Mason Dinosaur Quarry, Hell Creek Formation (Upper Cretaceous), South Dakota. M. S. thesis, University of Wisconsin, Madison, Wisconsin, 91 pp.
- Clemens, W. A., and J. H. Hartman. 2014. From *Tyrannosaurus rex* to asteroid impact: early studies (1901–1980) of the Hell Creek Formation in its type area; pp. 1–88 in G. P. Wilson, W. A. Clemens, J. R. Horner, and J. H. Hartman (eds.), Through the End of the Cretaceous in the Type Locality of the Hell Creek Formation in Montana and Adjacent Areas. Geological Society of America Special Papers 503, Boulder, Colorado.
- Colson, M. C., R. O. Colson, and R. Nellermoe. 2004. Stratigraphy and depositional environments of the upper Fox Hills and lower Hell Creek Formations at the Concordia Hadrosaur Site in northwestern South Dakota. Rocky Mountain Geology 39:93–111.
- Cope, E. D. 1869. Synopsis of the extinct Batrachia, Reptilia, and Aves of North America. Transactions of the American Philosophical Society 14:1–252.
- Dewaele, L., K. Tsogtbaatar, R. Barsbold, G. Garcia, K. Stein, F. Escuillie, and P. Godefroit. 2015. Perinatal specimens of *Sauropelodus angustirostris* (Dinosauria: Hadrosauridae), from the Upper Cretaceous of Mongolia. PLoS ONE 10:e0138806.

- Dilkes, D. W. 2000. Appendicular myology of the hadrosaurian dinosaur *Maiasaura peeblesorum* from the Late Cretaceous (Campanian) of Montana. *Transactions of the Royal Society of Edinburgh: Earth Sciences* 90:87–125.
- Dilkes, D. W. 2001. An ontogenetic perspective on locomotion in the Late Cretaceous dinosaur *Maiasaura peeblesorum* (Ornithischia: Hadrosauridae). *Canadian Journal of Earth Sciences* 38:1205–1227.
- Dodson, P. 1975. Taxonomic implication of relative growth in lambeosaurine hadrosaurs. *Systematic Zoology* 24:37–54.
- Dollo, L. 1888. Iguanodontidae et Camptonotidae. *Comptes Rendus hebdomadaires de l'Académie des Sciences, Paris* 106:775–777.
- Erickson, G. M., and T. A. Tumanova. 2000. Growth curve of *Psittacosaurus mongoliensis* Osborn (Ceratopsia: Psittacosauridae) inferred from long bone histology. *Zoological Journal of the Linnean Society* 130:551–566.
- Evans, D. C. 2010. Cranial anatomy and systematics of *Hypacrosaurus altispinus*, and a comparative analysis of skull growth in lambeosaurine hadrosaurids (Dinosauria: Ornithischia). *Zoological Journal of the Linnean Society* 159:398–434.
- Evans, D. C., C. A. Forster, and R. R. Reisz. 2005. The type specimen of *Tetragonosaurus erectofrons* (Ornithischia: Hadrosauridae) and the identification of juvenile lambeosaurines; pp. 349–366 in P. J. Currie and E. B. Koppelhus (eds.), *Dinosaur Provincial Park: A Spectacular Ancient Ecosystem Revealed*. Indiana University Press, Bloomington, Indiana.
- Farke, A. A., D. J. Chok, A. Herrero, B. Scolieri, and S. Werning. 2013. Ontogeny in the tube-crested dinosaur *Parasaurolophus* (Hadrosauridae) and heterochrony in hadrosaurids. *PeerJ* 1:e182.
- Fastovsky, D. E., and A. Bercovici. 2016. The Hell Creek Formation and its contribution to the Cretaceous-Paleogene extinction: a short primer. *Cretaceous Research* 57:368–390.
- Fiorillo, A. R., and R. S. Tykoski. 2016. Small hadrosaur manus and pes tracks from the Lower Cantwell Formation (Upper Cretaceous) Denali National Park, Alaska: implications for locomotion in juvenile hadrosaurs. *Palaios* 31:479–482.
- Freedman Fowler, E., and J. R. Horner. 2015. A new brachylophosaurin hadrosaur (Dinosauria: Ornithischia) with an intermediate nasal crest from the Campanian Judith River Formation of northcentral Montana. *PLoS ONE* 10:e0141304.
- Garstka, W. R., and D. A. Burnham. 1997. Posture and stance of *Triceratops*: evidence of a digitigrade manus and cantilever vertebral column; pp. 385–391 in D. L. Wolberg, E. Stump, and G. D. Rosenberg (eds.), *Dinofest International*. Philadelphia Academy of Natural Science, Philadelphia, Pennsylvania.
- Gilmore, C. W. 1924. A new species of hadrosaurian dinosaur of the Edmonton formation (Cretaceous) of Alberta, Canada. *Bulletin of the Department of Mines, Geological Survey of Canada, Geological Series* 43:38:13–26.
- Goodwin, M. B., and D. C. Evans. 2016. The early expression of squamosal horns and parietal ornamentation confirmed by new end-stage juvenile *Pachycephalosaurus* fossils from the Upper Cretaceous Hell Creek Formation, Montana. *Journal of Vertebrate Paleontology*. doi: 10.1080/02724634.2016.1078343.
- Goodwin, M. B., and J. R. Horner. 2014. Cranial morphology of a juvenile *Triceratops* skull from the Hell Creek Formation, McCone County, Montana, with comments on the fossil record of ontogenetically younger skulls; pp. 333–348 in G. P. Wilson, W. A. Clemens, J. R. Horner, and J. H. Hartman (eds.), *Through the End of the Cretaceous in the Type Locality of the Hell Creek Formation in Montana and Adjacent Areas*. Geological Society of America Special Papers 503, Boulder, Colorado.
- Goodwin, M. B., W. A. Clemens, J. R. Horner, and K. Padian. 2006. The smallest known *Triceratops* skull: new observations on ceratopsid cranial anatomy and ontogeny. *Journal of Vertebrate Paleontology* 26:103–112.
- Guenther, M. F. 2009. Influence of sequence heterochrony on hadrosaurid dinosaur postcranial development. *The Anatomical Record* 292:142–1441.
- Guenther, M. F. 2014. Comparative ontogenies (appendicular skeleton) for three hadrosaurids and a basal iguanodontian: divergent developmental pathways in Hadrosaurinae and Lambeosaurinae; pp. 398–415 in D. A. Eberth and D. C. Evans (eds.), *Hadrosaurs*. Indiana University Press, Bloomington, Indiana.
- Hartman, J. H. 2002. The Hell Creek Formation and the early picking of the Cretaceous-Tertiary boundary in the Williston Basin; pp. 1–8 in J. H. Hartman, K. R. Johnson, and D. J. Nichols (eds.), *The Hell Creek Formation and the Cretaceous-Tertiary Boundary in the Northern Great Plains: An Integrated Continental Record of the End of the Cretaceous*. Geological Society of America Special Papers 361, Boulder, Colorado.
- Holliday, C. M., R. C. Ridgely, J. C. Sedlmayr, and L. M. Witmer. 2010. Cartilaginous epiphyses in extant archosaurs and their implications for reconstructing limb function in dinosaurs. *PLoS ONE* 5:e13120.
- Horner, J. R. 1999. Egg clutches and embryos of two hadrosaurian dinosaurs. *Journal of Vertebrate Paleontology* 19:607–611.
- Horner, J. R., and P. J. Currie. 1994. Embryonic and neonatal morphology and ontogeny of a new species of *Hypacrosaurus* (Ornithischia, Lambeosauridae) from Montana and Alberta; pp. 312–336 in K. Carpenter, K. F. Hirsch, and J. R. Horner (eds.), *Dinosaur Eggs and Babies*. Cambridge University Press, Cambridge, U.K.
- Horner, J. R., M. B. Goodwin, and N. Myhrvold. 2011. Dinosaur census reveals abundant *Tyrannosaurus* and rare ontogenetic stages in the Upper Cretaceous Hell Creek Formation (Maastrichtian), Montana, USA. *PLoS ONE* 6:e16574.
- Horner, J. R., A. de Ricqlès, and K. Padian. 2000. Long bone histology of the hadrosaurid dinosaur *Maiasaura peeblesorum*: growth dynamics and physiology based on an ontogenetic series of skeletal elements. *Journal of Vertebrate Paleontology* 20:115–129.
- Horner, J. R., D. B. Weishampel, and C. A. Forster. 2004. Hadrosauridae; pp. 438–463 in D. B. Weishampel, P. Dodson, and H. Osmólska (eds.), *The Dinosauria*. University of California Press, Berkeley, California.
- Hutchinson, J. R., K. T. Bates, J. Molnar, V. Allen, and P. J. Makovicky. 2014. A computational analysis of limb and body dimensions in *Tyrannosaurus rex* with implications for locomotion, ontogeny, and growth. *PLoS ONE* 6:e26037.
- Jackson, F. D., and D. J. Varricchio. 2016. Fossil egg and eggshells from the Upper Cretaceous Hell Creek Formation, Montana. *Journal of Vertebrate Paleontology*. doi: 10.1080/02724634.2016.1185432.
- Keenan, S. W., and J. B. Scannella. 2014. Paleobiological implications of a *Triceratops* bonebed from the Hell Creek Formation, Garfield County, northeastern Montana; pp. 349–364 in G. P. Wilson, W. A. Clemens, J. R. Horner, and J. H. Hartman (eds.), *Through the End of the Cretaceous in the Type Locality of the Hell Creek Formation in Montana and Adjacent Areas*. Geological Society of America Special Papers 503, Boulder, Colorado.
- Kilbourne, B. M., and P. J. Makovicky. 2010. Limb bone allometry during postnatal ontogeny in non-avian dinosaurs. *Journal of Anatomy* 217:135–152.
- Lambe, L. M. 1917. A new genus and species of crestless hadrosaur from the Edmonton Formation of Alberta. *The Ottawa Naturalist* 31:65–73.
- Legendre, P. 2008. Model II regression. 1.6-3 ed CRAN.
- Livingston, V. J., M. F. Bonnan, R. M. Elsey, J. L. Sandrik, and D. R. Wilhite. 2009. Differential limb scaling in the American alligator (*Alligator mississippiensis*) and its implications for archosaur locomotor evolution. *The Anatomical Record* 292:787–797.
- Lyson, T. R., and N. R. Longrich. 2011. Spatial niche partitioning in dinosaurs from the latest Cretaceous (Maastrichtian) of North America. *Proceeding of the Royal Society B, Biological Sciences* 278:1158–1164.
- Maidment, S. C. R., and P. M. Barrett. 2014. Osteological correlates for quadrupedality in ornithischian dinosaurs. *Acta Palaeontologica Polonica* 59:53–70.
- Maidment, S. C. R., K. T. Bates, and P. M. Barrett. 2014. Three-dimensional computational modeling of pelvic locomotor muscle moment arms in *Edmontosaurus* (Dinosauria, Hadrosauridae) and comparisons with other archosaurs; pp. 433–448 in D. A. Eberth and D. C. Evans (eds.), *Hadrosaurs*. Indiana University Press, Bloomington, Indiana.
- Marsh, O. C. 1881. Principal characters of the American Jurassic dinosaurs, Part IV. *American Journal of Science* 21:417–423.
- Marsh, O. C. 1892. Notice of new reptiles from the Laramie Formation. *American Journal of Science, Series 3* 43:449–453.
- Maryańska, T., and H. Osmólska. 1984. Postcranial anatomy of *Sauropelodus angustirostris* with comments on other hadrosaurs. *Palaeontologica Polonica* 46:119–141.
- Mathews, J. C., S. L. Brusatte, S. A. Williams, and M. D. Henderson. 2009. The first *Triceratops* bonebed and its implications for gregarious behavior. *Journal of Vertebrate Paleontology* 29:286–290.
- McGarry, C. T., N. E. Campione, and D. C. Evans. 2013. Cranial anatomy and variation in *Prosauropodus maximum* (Dinosauria: Hadrosauridae). *Zoological Journal of the Linnean Society* 167:531–568.

- Pearson, D. A., T. Schaefer, K. R. Johnson, D. J. Nichols, and J. P. Hunter. 2002. Vertebrate biostratigraphy of the Hell Creek Formation in southwestern North Dakota and northwestern South Dakota; pp. 145–168 in J. H. Hartman, K. R. Johnson, and D. J. Nichols (eds.), The Hell Creek Formation and the Cretaceous-Tertiary Boundary in the Northern Great Plains: An Integrated Continental record of the End of the Cretaceous. Geological Society of America Special Papers 361, Boulder, Colorado.
- Prieto-Marquez, A. 2010. Global phylogeny of Hadrosauridae (Dinosauria: Ornithopoda) using parsimony and Bayesian methods. *Zoological Journal of the Linnean Society* 159:435–502.
- Prieto-Márquez, A. 2011. Cranial and appendicular ontogeny of *Bactrosaurus johnsoni*, a hadrosauroid dinosaur from the Late Cretaceous of northern China. *Palaeontology* 54:773–792.
- Prieto-Márquez, A. 2014. A juvenile *Edmontosaurus* from the late Maastrichtian (Cretaceous) of North America: implications for ontogeny and phylogenetic inference in saurolophine dinosaurs. *Cretaceous Research* 50:282–303.
- Rahn, H., P. Parisi, and C. V. Paganelli. 1982. Estimating the initial density of birds' eggs. *The Condor* 84:339–341.
- Rasband, W. S. 1997. Image J. U.S. National Institutes of Health, Bethesda, Maryland. Available at: <http://imagej.nih.gov/ij/>. Accessed March 3, 2017.
- R Development Core Team. 2016. R: a language and environment for statistical computing. Version 3.3.1. Vienna, Austria: R Foundation for Statistical Computing.
- Reisz, R. R., D. Scott, H.-D. Sues, D. C. Evans, and M. A. Raath. 2005. Embryos of an Early Jurassic prosauropod dinosaur and their evolutionary significance. *Science* 309:761–764.
- Russell, D. A., and M. Manabe. 2002. Synopsis of the Hell Creek (uppermost Cretaceous) dinosaur assemblage; pp. 169–176 in J. H. Hartman, K. R. Johnson, and D. J. Nichols (eds.), The Hell Creek Formation and the Cretaceous-Tertiary Boundary in the Northern Great Plains: An Integrated Continental Record of the End of the Cretaceous. Geological Society of America Special Papers 361, Boulder, Colorado.
- Scannella, J. B., and D. W. Fowler. 2014. A stratigraphic survey of *Triceratops* localities in the Hell Creek Formation, northeastern Montana (2006–2010); pp. 313–332 in G. P. Wilson, W. A. Clemens, J. R. Horner, and J. H. Hartman (eds.), Through the End of the Cretaceous in the Type Locality of the Hell Creek Formation in Montana and Adjacent Areas. Geological Society of America Special Papers 503, Boulder, Colorado.
- Seeley, H. G. 1887. On the classification of the fossil animals commonly named Dinosauria. *Proceedings of the Royal Society of London* 43:165–171.
- Sprain, C. J., P. R. Renne, G. P. Wilson, and W. A. Clemens. 2015. High-resolution chronostratigraphy of the terrestrial Cretaceous-Paleogene transition and recovery interval in the Hell Creek region, Montana. *Geological Society of America Bulletin* 127:393–409.
- Tokaryk, T. T. 1997. First evidence of juvenile ceratopsians (Reptilia: Ornithischia) from the Frenchman Formation (late Maastrichtian) of Saskatchewan. *Canadian Journal of Earth Sciences* 34:1401–1404.
- Warton, D. I., I. J. Wright, D. S. Falster, and M. Westoby. 2006. Bivariate line-fitting methods for allometry. *Biological Reviews* 81:259–291.
- Woodward, H. N., E. A. Freedman Fowler, J. O. Farlow, and J. R. Horner. 2015. *Maiasaura*, a model organism for extinct vertebrate population biology: a large sample statistical assessment of growth dynamics and survivorship. *Paleobiology* 41:503–527.
- Xing, H., J. C. Mallon, and M. L. Currie. 2017. Supplementary cranial description of the types of *Edmontosaurus regalis* (Ornithischia: Hadrosauridae), with comments on the phylogenetics and biogeography of Hadrosaurinae. *PLoS ONE* 12:e0175253.
- Xing, H., X. Zhao, K. Wang, D. Li, S. Chen, J. C. Mallon, Y. Zhang, and X. Xu. 2014. Comparative osteology and phylogenetic relationships of *Edmontosaurus* and *Shantungosaurus* (Dinosauria: Hadrosauridae) from the Upper Cretaceous of North America and East Asia. *Acta Geologica Sinica* 88:1623–1652.
- Zhao, Q., M. J. Benton, C. Sullivan, P. M. Sander, and X. Xu. 2013. Histology and postural change during the growth of the ceratopsian dinosaur *Psittacosaurus lujiatunensis*. *Nature Communications* 4:2079.

Submitted April 25, 2017; revisions received July 21, 2017; accepted July 21, 2017.

Handling editor: Richard Butler.